Molecular Pharmacology Fast Forward. Published on November 30, 2018 as DOI: 10.1124/mol.118.113233
This article has not been copyedited and formatted. The final version may differ from this version.

MOL#113233

The Cannabinoid CB2 agonist AM1710 differentially suppresses distinct pathological pain states and attenuates morphine tolerance and withdrawal

Ai-Ling Li, Xiaoyan Lin, Amey S. Dhopeshwarkar, Ana Carla Thomaz, Lawrence M. Carey, Yingpeng Liu, Spyros P. Nikas, Alexandros Makriyannis, Ken Mackie and Andrea G. Hohmann

Department of Psychological and Brain Sciences, Indiana University, Bloomington, IN, United States (A-L L., X. L., A.S.D., A.C.T., L.M.C., K.M., A.G.H.)

Program in Neuroscience, Indiana University, Bloomington, IN, United States (A.C.T., L.M.C., K.M., A.G.H.)

Genome, Cell and Developmental Biology Program, Indiana University, Bloomington, IN, United States (A.C.T., A.G.H)

Center for Drug Discovery, Northeastern University, Boston, MA (Y.L., S.N., A.M.)

Gill Center for Biomolecular Science, Indiana University, Bloomington, IN, United States (K.M., A.G.H.)

Molecular Pharmacology Fast Forward. Published on November 30, 2018 as DOI: 10.1124/mol.118.113233
This article has not been copyedited and formatted. The final version may differ from this version.

Running Title

Evaluation of CB2 agonist AM1710

Corresponding author: Andrea G Hohmann, Psychological and Brain Sciences, Gill Center for Biomolecular Sciences, Indiana University, Bloomington, IN 47405, USA. Email: hohmanna@indiana.edu. Telephone: 812-856-0672.

Number of text pages: 40

Number of figures: 9

Number of references: 45

Abstract word count: 248

Introduction word count: 674

Discussion word count: 1497

Abbreviations: AM1710, 3-(1, 1-dimethyl-heptyl)-1-hydroxy-9-methoxy-benzo(c) chromen-6-one; BSA, bovine serum albumin; CB1, cannabinoid receptor 1; CB2, cannabinoid receptor 2; CFA, complete Freund's adjuvant; CNS, central nervous system; CP55940, (2)-cis-3-[2-hydroxy-4-(1,1-dimethylheptyl)- phenyl]-trans-4-(3-hydroxypropyl)cyclohexanol; DMSO, dimethylsufoxide; ERK, extracellular signal-regulated kinases; HEK, human embryonic kidney; hCB2, human cannabinoid receptor 1; IP1, myo-inositol phosphate 1; KO, knockout; LY2828360, (8-(2-chlorophenyl)-2-methyl-6-(4-methylpiperazin-1-yl)- 9-(tetrahydro-2H-pyran-4-yl)-9H-purine); mCB2, mouse cannabinoid receptor 2; pERK 1/2, phosphorylated ERK1/2; PSNL, partial sciatic nerve ligation; PTX, pertussis toxin; TBS, Tris-buffered saline; Δ^9-THC, Δ^9-tetrahydrocannabinoil; WT, wild type.

Molecular Pharmacology Fast Forward. Published on November 30, 2018 as DOI: 10.1124/mol.118.113233
This article has not been copyedited and formatted. The final version may differ from this version.

ABSTRACT

AM1710, a cannabilactone CB2 agonist, suppresses chemotherapy-induced neuropathic pain in rodents without producing tolerance or unwanted side effects associated with CB1 receptors. However, the signaling profile of AM1710 remains incompletely characterized. It is not known whether AM1710 behaves as a broad spectrum analgesic and/or suppresses the development of opioid tolerance and physical dependence. In vitro, AM1710 inhibited forskolin-stimulated cAMP production and produced enduring activation of ERK1/2 phosphorylation in HEK cells stably expressing mCB2. Only modest species differences in the signaling profile of AM1710 were observed between HEK cells stably expressing mCB2 and hCB2. In vivo, AM1710 produced a sustained inhibition of paclitaxel-induced allodynia in mice. In paclitaxel-treated mice, prior history of AM1710 treatment (5 mg/kg/day x 12 day, i.p.) delayed the development of antinociceptive tolerance to morphine and attenuated morphine-induced physical dependence. AM1710 (10 mg/kg, i.p.) did not precipitate CB1 receptor-mediated withdrawal in mice rendered tolerant to Δ^9-tetrahydrocannabinol, suggesting that AM1710 is not a functional CB1 antagonist *in vivo*. Furthermore, AM1710 (1, 3, 10 mg/kg, i.p.) did not suppress established mechanical allodynia induced by complete Freund's adjuvant (CFA) or by partial sciatic nerve ligation (PSNL). Similarly, prophylactic and chronic dosing with AM1710 (10 mg/kg, i.p.) did not produce anti-allodynic efficacy in the CFA model. By contrast, gabapentin suppressed allodynia in both CFA and PSNL models. Our results indicate that AM1710 is not a broad spectrum analgesic agent in mice and suggest the need to identify signaling pathways underlying CB2 therapeutic efficacy to identify appropriate indications for clinical translation.

Keywords: CB2 agonist, AM1710, anti-allodynia, morphine tolerance, morphine dependence, inflammatory pain, neuropathic pain

Molecular Pharmacology Fast Forward. Published on November 30, 2018 as DOI: 10.1124/mol.118.113233
This article has not been copyedited and formatted. The final version may differ from this version.

INTRODUCTION

The opioid epidemic has intensified drug discovery efforts aimed at identifying efficacious alternatives to opioids that lack their undesirable properties. Opioids suppress diverse forms of pain, but chronic use results in tolerance and physical dependence (Yekkirala *et al.*, 2017). Cannabinoids represent an alternative to opioid analgesics (Pertwee, 2001). There are two well characterized cannabinoid receptors: CB1 is abundantly expressed in the central nervous system (CNS) (Herkenham *et al.*, 1991; Matsuda *et al.*, 1993) and CB2 is predominantly expressed in immune cells and in the periphery (Galiegue *et al.*, 1995). CB2 receptors may, nevertheless, be induced in the central nervous system (CNS) under pathological conditions (Zhang *et al.*, 2003; Beltramo *et al.*, 2006; Atwood and Mackie, 2010). CB2 receptor activation does not produce unwanted CNS-mediated side effects associated with CB1 (Malan *et al.*, 2003; Guindon and Hohmann, 2008; Deng, Guindon, *et al.*, 2015). We recently reported that the G protein-biased CB2 agonist LY2828360 suppressed chemotherapy-induced neuropathic pain and attenuated development of morphine tolerance and physical dependence in neuropathic mice (Lin *et al.*, 2017). Whether such effects are specific to LY2828360, or translate more broadly to other CB2 agonists with different signaling profiles remains unknown.

AM1710, a cannabilactone CB2 agonist, exhibits 54-fold selectivity for CB2 over CB1 (Khanolkar *et al.*, 2007; Rahn *et al.*, 2011) and lacks off-target activity at 63 sites evaluated (Rahn *et al.*, 2011). However, AM1710 was recently found to be a low potency CB1 inverse agonist *in vitro* (Dhopeshwarkar *et al.*, 2017), but the *in vivo* functional impact of this is unknown. We first characterized the signaling profile of AM1710 *in vitro.* Unlike CB1, which is largely conserved across diverse species, sequence heterogeneity in CB2 has been noted across species (Griffin et al., 2000; Brown et al., 2002; Bingham et al., 2007), which could lead to different pharmacological responses to identical drugs (Mukherjee et al., 2004; Bingham et al., 2007). For example, R,S-AM1241 is an agonist at human CB2, but is an inverse agonist at rat and mouse CB2 (Bingham et al., 2007). Consequently, caution must be taken when extrapolating effects observed in rodent

Molecular Pharmacology Fast Forward. Published on November 30, 2018 as DOI: 10.1124/mol.118.113233
This article has not been copyedited and formatted. The final version may differ from this version.

models to humans. Therefore, in this study, we first characterized the in vitro signaling profile of AM1710 using both mouse and human CB2 receptors.

We validated antinociceptive efficacy of AM1710 and evaluated whether AM1710 could attenuate morphine tolerance and naloxone-precipitated opioid withdrawal in paclitaxel-treated mice as reported previously for LY2828360 (Lin *et al.*, 2017). We also evaluated whether AM1710 acts as a functional CB1 antagonist *in vivo* by challenging mice treated chronically with Δ^9-tetrahydrocannabinol (Δ^9-THC) with AM1710 or rimonabant to precipitate CB1-dependent cannabinoid withdrawal.

Finally, we evaluated whether AM1710 is a broad-spectrum analgesic, efficacious across mechanistically distinct inflammatory and neuropathic pain models. AM1710 exhibits antinociceptive efficacy in multiple pre-clinical models of neuropathic pain (Deng *et al.*, 2012; Wilkerson *et al.*, 2012; Rahn *et al.*, 2014; Deng, Guindon, *et al.*, 2015). Despite the promising preclinical therapeutic potential of AM1710, whether AM1710 is efficacious across mechanistically distinct inflammatory and neuropathic pain models remains poorly understood. This evaluation is crucial because our recent studies suggest that the anti-allodynic efficacy of the CB2-preferring agonist GW405833 is CB1-mediated and not CB2-mediated (Li *et al.*, 2017). Therefore, a secondary goal of this study was to characterize possible antihyperalgesic effects of AM1710 in models of inflammatory pain induced by intraplantar injection of complete Freund's adjuvant (CFA) and neuropathic pain induced by partial sciatic nerve ligation (PSNL) in mice. We compared the antinociceptive efficacy of AM1710 to gabapentin, which shows efficacy in both models (Patel *et al.*, 2001). To verify whether engagement of CB2 by a structurally distinct cannabinoid with a different *in vitro* signaling profile was antiallodynic in these two pain models, we administered the mixed CB1/CB2 agonist CP55940 to CB1 KO mice. CP55940 binds to CB1 and CB2 with similar affinities *in vitro* (Felder *et al.*, 1995) and does not exhibit functionally biased signaling at CB2 (Atwood *et al.*, 2012). We previously showed that high doses of CP55940 (10

Molecular Pharmacology Fast Forward. Published on November 30, 2018 as DOI: 10.1124/mol.118.113233
This article has not been copyedited and formatted. The final version may differ from this version.

mg/kg, i.p.) produced CB2-mediated anti-allodynia in paclitaxel-treated CB1 KO mice (Deng, Cornett, *et al.*, 2015).

MATERIALS AND METHODS

Animals

Adult mice (25-35g) were used in this study. Number, strain and sex of animals are indicated for each group in the figure legends. CB2 KO mice (bred at Indiana University) and wildtype (WT) on a C57BL/6J background (bred at Indiana University or purchased from The Jackson Laboratory, Bar Harbor, ME), and CB1 KO mice (bred at Indiana University) on a CD1 background and CD1 wildtype controls ((bred at Indiana University or purchased from Charles River Laboratories, Wilmington, MA) were included. Animals were single-housed at relatively constant temperature (73±2^{o}F) and humidity (45%) under light-dark cycles of 12/12 h. All the experimental procedures were approved by Bloomington Institutional Animal Care and Use Committee of Indiana University and followed the guidelines for the treatment of animals of the International Association for the Study of Pain (Zimmermann, 1983).

Chemicals

AM1710 (Khanolkar *et al.*, 2007) was synthesized in the Makriyannis lab by S.N, and Y.L. (Boston, MA, USA); CP55940 was purchased from Cayman Chemical Company or was obtained from National Institute of Drug Abuse Drug Supply Service (Bethesda, MD). AM1710, morphine (Sigma-Aldrich) and CP55940 were dissolved in a vehicle containing dimethylsulfoxide (Sigma-Aldrich, St. Louis, MO), emulphor (Alkamuls EL 620L, Solvay, Princetone, NJ), ethanol (Sigma-Aldrich), and 0.9% saline (Aquilite System, Hospira Inc, Lake Forest, IL) at a ratio of 5:2:2:16. Gabapentin (Spectrum Chemical, NJ, USA) or naloxone (Sigma-Aldrich) were dissolved in 0.9% saline. Paclitaxel (Tecoland Corporation, Irvine, CA, USA) was dissolved in a cremophor-based vehicle made of Cremophor EL (Sigma-Aldrich, St. Louis, MO), ethanol, 0.9% saline at ratio of 1:1:18 as described previously (Deng, *et al.*, 2015). Δ^{9}-THC (National Institute on Drug abuse)

Molecular Pharmacology Fast Forward. Published on November 30, 2018 as DOI: 10.1124/mol.118.113233
This article has not been copyedited and formatted. The final version may differ from this version.

was dissolved in a vehicle of 95% ethanol, Cremophor and sterile saline in a ratio of 1:1:18 respectively. Drugs were delivered via intraperitoneal injection (i.p.) to mice in a volume of 5 ml/kg or 10 ml/kg.

Cell Culture

HEK293 cells stably expressing mouse CB2 (HEK mCB2) or human CB2 (HEK hCB2) receptors were generated, expanded and maintained in Dulbecco's Modified Eagle media with 10% fetal bovine serum and penicillin/streptomycin (GIBCO, Carlsbad, CA) at 37 °C in 5% CO_2 (Atwood *et al.*, 2012). For ease of immunostaining, an amino-terminal hemagglutinin epitope tag was introduced into the CB2 receptor (Atwood *et al.*, 2012).

Forskolin-Stimulated cAMP Accumulation Assay

Forskolin-stimulated cAMP accumulation assays were optimized using Perkin Elmer's LANCE® ultra cAMP kit (Catalog # TRF0262, Perkin Elmer, Boston, MA) as per the manufacturer's instructions. All assays were performed at room temperature using 384-optiplates (Catalog# 6007299, Perkin Elmer). Briefly, cells were resuspended in 1X stimulation buffer (1X Hank's Balanced Salt Solution, 5 mM HEPES, 0.5 mM IBMX, 0.1% BSA, pH 7.4, made fresh on the day of experiment). Cells (HEK transfected with mouse and human CB2) were incubated for 1 hour at 37°C, 5% CO_2 and humidified air and then transferred to a 384-optiplate (500 cells/µl, 10µl), followed by stimulation with drugs/compounds and forskolin (1µM final concentration) (as indicated) prepared in 1X stimulation buffer, for defined time points. Cells-only wells were treated as basal. No forskolin, no drug and drug-only (no forskolin) controls for every defined time point were also included. For experiments involving pertussis toxin (PTX), cells were incubated overnight with 100 ng/ml PTX at 37° C, 5% CO2 and humidified air. After stimulation for the appropriate time, cells were lysed by addition of 10µl Eu-cAMP tracer working solution (4X, made fresh in 1X lysis buffer supplied with the kit; under subdued light conditions) and 10 µl *Ulight*™ anti-cAMP working solution (4X, made fresh in 1X lysis buffer) and further incubated for 1 hour at

Molecular Pharmacology Fast Forward. Published on November 30, 2018 as DOI: 10.1124/mol.118.113233
This article has not been copyedited and formatted. The final version may differ from this version.

room temperature. Plates were then read in the TR FRET mode on an Enspire plate reader (Perkin Elmer, Boston, MA). Assays were performed in triplicate, unless otherwise mentioned.

Detection of phosphorylated ERK1/2 and JNK

HEK mouse and human CB2 cells were seeded on poly-D-lysine coated 96-well plates (75,000 cells/well) and grown overnight at 37 °C, 5% CO_2, humidified air. For pertussis toxin (PTX)-treated experiments, cells were treated overnight with 100 ng/ml PTX at 37 ^oC, 5% CO_2, humidified air. The following day, cells were serum starved for 5 hours at 37 ^oC, 5% CO_2, humidified air. The medium was then replaced by HBS/BSA (0.2 mg/ml) and cells were challenged with drugs/compounds for the indicated time. Wells containing cells only were treated as basal (control) condition. After drug incubation, plates were emptied and quickly fixed with ice cold 4% paraformaldehyde for 20 mins, followed by ice-cold methanol with the plate maintained at -20°C for 15 min. Plates were then washed with TBS/0.1% Triton X-100 for 25 mins (5 x 5 min washes). The wash solution was then replaced by Odyssey blocking buffer and incubated further for 90 min with gentle shaking at room temperature. Blocking solution was then removed and replaced with blocking solution containing anti-phospho-ERK1/2 (p44/42) antibody or total ERK1/2 (1:150; Antibody # 9101 or 9102 respectively, Cell Signaling Technology®, Danvers, MA) and was shaken overnight at 4°C. For the JNK assay, blocking solution was replaced with blocking solution containing anti-phospho JNK (P46/54) antibody (1:100; Antibody # 9251, Cell Signaling Technology®, Danvers, MA). The next day, plates were washed with TBS containing 0.05% Tween-20 for 25 min (5x 5 min washes). Secondary antibody, donkey anti-rabbit conjugated with IR800 dye (Rockland, Limerick, PA), prepared in blocking solution, was added and gently shaken for 1 hour at room temperature. The plates were then again washed 5 times with TBS/0.05% Tween-20 solution. The plates were patted dry and scanned using LI-COR Odyssey scanner. pERK1/2 activation (expressed in %) were calculated by dividing average integrated intensities of the drug treated wells by average integrated intensities of vehicle-treated wells. All assays were performed in triplicate, unless otherwise mentioned.

Molecular Pharmacology Fast Forward. Published on November 30, 2018 as DOI: 10.1124/mol.118.113233
This article has not been copyedited and formatted. The final version may differ from this version.

Partial Sciatic Nerve Ligation (PSNL)-Induced Neuropathic Pain

PSNL was performed as described in our previously published work (Li *et al.*, 2017). Briefly, under isoflurane anesthesia, a longitudinal incision (1-1.5 cm) was made in the proximal right thigh to expose the sciatic nerve. One third to one half of the sciatic nerve was ligated just above its trifurcation using 8-0 silk suture (Sharpoint DA-2526N, Reading, PA). The incision was then closed in layers. Animals were allowed at least two weeks to recover and fully develop neuropathic pain.

Complete Freund's Adjuvant (CFA)-Induced Inflammatory Pain

CFA was diluted with an equal volume of sterile saline and 20 µl of this mixture was injected subcutaneously into the plantar surface of the right hind paw.

Paclitaxel-Induced Peripheral Neuropathic Pain

Paclitaxel (4 mg/kg, i.p.) was administered to animals four times on alternate days (cumulative dose, 16 mg/kg, i.p.) to induce painful peripheral neuropathy, as previously described by our group (Deng, Guindon, *et al.*, 2015).

Assessment of Mechanical Allodynia

As previously described (Li *et al.*, 2017), mice were placed in individual transparent Plexiglass chambers on an elevated mesh platform and allowed to habituate for minimum of 30 minutes prior to testing. A semi-flexible tip connected to an electronic von Frey anesthesiometer (IIITC Life Science Inc., Woodland Hills, CA) was applied vertically to the midplantar region of the hind paw with gradually increased force. The force in grams when animal withdrew the paw was recorded. Each paw was tested twice with a several minute interval between stimulations to avoid sensitization. Mechanical paw withdrawal thresholds in grams (g) were averaged respectively for each paw for mice subjected to a unilateral PSNL or CFA injection. In paclitaxel-treated mice where allodynia is observed bilaterally in each paw, paw withdrawal thresholds were calculated

Molecular Pharmacology Fast Forward. Published on November 30, 2018 as DOI: 10.1124/mol.118.113233
This article has not been copyedited and formatted. The final version may differ from this version.

for each paw as described above and subsequently averaged across paws, to obtain a single dependent measure per animal for each stimulus modality at a given timepoint.

Assessment of Cold Allodynia

Duration of responding to cold (seconds) was assessed after the assessment of responsiveness to mechanical stimulation for pain models in which cold allodynia is prominent, as we have previously published (Lin *et al.*, 2017). A 1 ml syringe with needle removed was filled with acetone (Sigma-Aldrich). An acetone bubble (5-6 µl) was formed at the tip of the syringe by applying slight pressure to the plunger. The acetone bubble was then gently applied to the plantar surface of the hind paw with care taken to avoid contacting the paw with the syringe tip and applying mechanical pressure. The time in seconds spent attending to (i.e., elevating, biting, licking, shaking or flinching) the paw stimulated with acetone was measured in triplicate for each paw.

Evaluation of Opioid or CB1 Receptor-Mediated Withdrawal Symptoms

Naloxone-precipitated opioid withdrawal. C57BL/6J mice receiving either vehicle or morphine alone (10 mg/kg/day, i.p.) or a combination of morphine with AM1710 were first challenged with vehicle (0.9% saline, i.p.) 30 minutes after the last treatment. Thirty minutes after the vehicle challenge, animals were then challenged with naloxone (5 mg/kg, i.p.) to induce opioid withdrawal. Mice were videotaped, and the number of jumps was scored in 5-minute intervals for a total observation period of 30 minutes after challenge with either vehicle or naloxone.

Rimonabant-precipitated cannabinoid CB1 receptor-dependent withdrawal. Naïve C57BL/6J mice received once daily injections of Δ^9-THC (50 mg/kg, i.p.) for 9 days. Thirty minutes after the last injection of Δ^9-THC on day 9, all animals were first challenged with vehicle. Then, 30 minutes after vehicle challenge, half of the animals received a second challenge with AM1710 (10 mg/kg, i.p.) and the other half of the animals received a second challenge with the CB1 antagonist rimonabant (10 mg/kg, i.p.). Behavior was videotaped for 30 minutes immediately

Molecular Pharmacology Fast Forward. Published on November 30, 2018 as DOI: 10.1124/mol.118.113233
This article has not been copyedited and formatted. The final version may differ from this version.

after vehicle, rimonabant, or AM1710 challenge. The numbers of front paw tremors, headshakes, grooming, and rearing behaviors were counted by investigator blinded to treatment conditions according to methods described in our previously published work (Li *et al.*, 2017).

General In Vivo Experimental Protocol

Mechanical and cold responsiveness was assessed 30 minutes after pharmacological manipulations.

Experiment 1. We investigated whether chronic pretreatment with AM1710 in Phase I was able to block the development of tolerance to morphine in Phase II in paclitaxel-treated mice. Male C57BL/J6 mice were injected with paclitaxel (4 mg/kg, i.p.) on alternate days on four occasions as described above to induce a painful peripheral neuropathy. After paclitaxel-induced neuropathic pain was fully established, mice were randomly assigned to one of three groups. The treatment period was composed of two phases, Phase I and Phase II, with four days separating the two phases. The protocol employed here was identical to that used in our previously published work to show that the G protein-biased CB2 agonist LY2828360 suppressed paclitaxel-induced neuropathic pain and blocked development of tolerance to morphine in paclitaxel-treated mice (Lin *et al.*, 2017). One group of mice received daily i.p. injections of AM1710 for 12 consecutive days (5 mg/kg/day, i.p.) during Phase I, followed by daily i.p. injections of morphine (10 mg/kg/day, i.p.) for 12 days during Phase II (i.e. AM1710 (I)-morphine (II)). A second group of mice received parallel daily injections of vehicle for 12 days during Phase I, followed by daily injections of morphine in Phase II (i.e. vehicle (I)-morphine (II)). A third group of mice received parallel daily vehicle administration in both Phase I and II (vehicle (I)-vehicle (II)). Mechanical and cold sensitivity were assessed on day 1, 4, 8, 12 in Phase I and day 16, 19, 23, 27 in Phase II.

At the end of all treatments, all mice were challenged (i.p.) with vehicle, followed by naloxone (i.p.), as described above, and withdrawal behaviors were recorded for 30 min following

Molecular Pharmacology Fast Forward. Published on November 30, 2018 as DOI: 10.1124/mol.118.113233
This article has not been copyedited and formatted. The final version may differ from this version.

each challenge. Changes in body temperature (° C) and body weight (g) induced by challenge with vehicle and naloxone, respectively, were also recorded at 30 min and 2 h post injection.

Experiment 2. We investigated whether AM1710 was able to precipitate CB1 receptor-mediated withdrawal in mice chronically treated with Δ^9-THC, consistent with our recent report that AM1710 may behave as CB1 antagonist *in vitro* (Dhopeshwarkar *et al.*, 2017). Naïve C57BL/6J mice received once daily dosing with Δ^9-THC (50 mg/kg/day, i.p.) for 9 days and were then challenged with vehicle, rimonabant or AM1710 as described above. The withdrawal behaviors were recorded for 30 min following each challenge as described in our previously published work (Li *et al.*, 2017).

Experiment 3. We assessed the dose response of AM1710 (1, 3, 10 mg/kg, i.p.) in suppressing established inflammatory pain induced by CFA using both WT and CB2 KO mice. The dose response of gabapentin in suppressing inflammatory nociception in the same pain model was assessed in WT mice, in parallel, as a positive control.

We further evaluated the anti-allodynic effect of prophylactic chronic treatment with AM1710 (10 mg/kg, i.p.) in mice receiving a unilateral intraplantar injection of CFA. Comparisons were made with gabapentin (50 mg/kg, i.p.) in C57BL/J6 mice. AM1710 (10 mg/kg, i.p.) or gabapentin (50 mg/kg, i.p.) was injected 30 minutes before CFA injection on day 1, and continued once daily for 12 consecutive days for AM1710 and for 8 consecutive days for gabapentin.

Experiment 4. We assessed the dose response of AM1710 (1, 3, 10 mg/kg, i.p.) in suppressing established neuropathic pain induced by PSNL using both WT and CB2 KO mice. The dose response of gabapentin in suppressing PSNL-induced neuropathic nociception was assessed in WT mice, in parallel, as a positive control.

Experiment 5. We evaluated whether CP55940 (3 and 10 mg/kg, i.p.) produced anti-allodynic effects through activation of CB2 receptors in CB1 KO mice subjected to PSNL-induced neuropathic pain and CFA-induced inflammatory pain.

Molecular Pharmacology Fast Forward. Published on November 30, 2018 as DOI: 10.1124/mol.118.113233
This article has not been copyedited and formatted. The final version may differ from this version.

Statistical Analysis

Two-way mixed ANOVA was used to analyze the main effect of time and main effect of groups, as well as interaction between time and groups. Two-way repeated measures ANOVA was employed for the analyses of main effect of time, main effect of paws, and interactions between time and paws. One-way ANOVA was used to detect the group differences where no time course was involved (e.g., group differences in jumping behavior after naloxone challenge). Bonferroni post hoc (for all comparisons) and Bonferroni's multiple comparison tests (for making a restricted set of comparisons) were performed for all pairwise comparisons. Planned comparison t tests (paired or unpaired, as appropriate) were employed for specific comparisons of interest as indicated. SPSS 24 (IBM Corporation, Armonk, NY) was used to analyze *in vivo* data; GraphPad Prism version 5.02 (GraphPad Software, San Diego, CA) was used to analyze *in vitro* data. $P < 0.05$ was considered statistically significant. Figures were generated using GraphPad Prism version 5.02 (GraphPad Software, San Diego, CA). Data are expressed as mean ± S.E.M.

RESULTS

AM1710 Inhibited Forskolin-Stimulated cAMP Accumulation in HEK Cells Expressing mCB2 or hCB2, but the Kinetics of Inhibition Differed Between mCB2 and hCB2.

In HEK cells stably expressing mCB2, cAMP levels differed between treatments ($F_{5, 12} = 609$, $p < 0.001$) and varied over time ($F_{4, 48} = 108.2$, $p < 0.001$) (fig. 1A). The interaction between treatment and time was significant ($F_{20, 48} = 44.58$, $p < 0.001$) (fig. 1A). Forskolin persistently increased cAMP levels in cells incubated with vehicle starting at 5 minutes ($p < 0.001$). The presence of CP55940 (1μM final concentration) ($p < 0.001$) or AM1710 (1μM final concentration) ($p < 0.001$) attenuated forskolin-induced cAMP levels at 5 minutes. Although CP55940 exhibited a stronger inhibitory effect than AM1710 at 5 minutes ($p < 0.001$), the inhibitory effect of AM1710 outlasted that of CP55940 and inhibition by the AM1710 dissipated by 15 minutes. Following the brief inhibition of cAMP levels by CP55940 or AM1710, cAMP levels exceeded those in cells treated

Molecular Pharmacology Fast Forward. Published on November 30, 2018 as DOI: 10.1124/mol.118.113233
This article has not been copyedited and formatted. The final version may differ from this version.

with forskolin alone ($p < 0.001$) (fig. 1A). In the absence of forskolin, CP55940 or AM1710 alone did not change cAMP levels, as no differences were observed between these conditions and the basal/no forskolin condition with one exception; AM1710 treatment alone decreased cAMP levels below the basal/no forskolin level at 10 minutes ($p = 0.012$). Pertussis toxin (PTX) pretreatment abolished the decrease in forskolin-stimulated cAMP induced by either CP55940 (1 μM final concentration) or AM1710 (1 μM final concentration) in HEK cells stably expressing mCB2 (fig. 1B). Despite the significant changes in cAMP over time ($F_{3, 24} = 29.51$, $p < 0.001$), differences between treatment ($F_{3, 8} = 1443$, $p < 0.001$) and interaction ($F_{9, 24} = 2.795$, $p = 0.021$), no differences were detected between treatments with forskolin stimulation at any time point in the PTX-treated cells ($p > 0.235$) (fig. 1B).

In HEK cells stably expressing hCB2, cAMP levels differed between treatments ($F_{5, 12} = 412.6$, $p < 0.001$) and varied over time ($F_{4, 48} = 123.9$, $p < 0.001$) (fig. 1C). The interaction between treatment and time was significant ($F_{20, 48} = 47.54$, $p < 0.001$) (fig. 1C). Similarly, forskolin persistently increased cAMP levels in cells incubated with vehicle starting at 5 minutes ($p < 0.001$). However, only CP55940 produced early inhibition of forskolin-induced cAMP levels at 5 minutes ($p < 0.001$) (fig. 1C). By contrast, AM1710 induced a delayed and persistent inhibition of forskolin-stimulated cAMP levels starting at 10 minutes ($p < 0.001$) (fig. 1C). Similar to the HEK cells stably expressing mCB2, CP55940 and AM1710 alone did not change the cAMP levels in cells stably expressing hCB2 ($p = 1$). PTX pretreatment blocked the inhibition of forskolin-stimulated cAMP produced by either CP55940 (1 μM final concentration) or AM1710 (1μM final concentration) in HEK cells stably expressing hCB2 (fig. 1D). Despite the significant changes over time ($F_{3, 24} = 22.95$, $p < 0.001$), differences between treatment ($F_{3, 8} = 2472$, $p < 0.001$) and interaction ($F_{9, 24} = 3.391$, $p = 0.008$), no differences were detected between treatments with forskolin stimulation at all time points ($p > 0.831$) with one exception; in the presence of forskolin, AM1710 increased cAMP levels compared to forskolin alone at 5 minutes in PTX-treated cells ($p = 0.048$) (fig. 1D)

Molecular Pharmacology Fast Forward. Published on November 30, 2018 as DOI: 10.1124/mol.118.113233
This article has not been copyedited and formatted. The final version may differ from this version.

AM1710 Activated ERK1/2 Phosphorylation in HEK Cells Expressing mCB2 or hCB2, but the Kinetics of Inhibition Differed Between mCB2 and hCB2.

In HEK cells stably expressing mCB2, phosphorylated ERK1/2 levels changed over time across the treatments ($F_{4, 32} = 157.7$, $p < 0.001$) (fig. 2A). Both CP55940 (1μM final concentration) and AM1710 (1μM final concentration) increased phosphorylated ERK1/2 levels ($F_{3, 8} = 969.4$, $p < 0.001$). This increase was time dependent ($F_{12, 32} = 50.43$, $p < 0.001$). Both AM1710 and CP55940 induced a rapid (starting at 5 minutes, $p < 0.001$) and long-lasting increase in ERK1/2 phosphorylation (up to 30 minutes, $p < 0.001$). The ERK1/2 phosphorylation induced by AM1710 was consistent throughout the observation interval, while CP55940-induced ERK1/2 phosphorylation was more variable and biphasic (fig. 2A). The basal level of ERK1/2 phosphorylation was slightly lower than that of the vehicle condition at 0 ($p = 0.01$) and 5 minutes ($p = 0.006$), but did not differ from vehicle at any of the remaining time points ($p > 0.764$). PTX pretreatment differentially affected ERK1/2 phosphorylation levels between treatments ($F_{3, 8} = 35.64$, $p < 0.001$) and over time ($F_{3, 24} = 167.8$, $p < 0.001$) (fig. 2B). A significant interaction between treatment and time was observed ($F_{9, 24} = 57.28$, $p < 0.001$) and PTX pretreatment abolished the rapid activation of ERK1/2 induced by AM1710 (1μM final concentration) at 5 minutes (fig. 2B). Interestingly, after PTX pretreatment, ERK1/2 was dephosphorylated by 5 minutes of CP55940 treatment relative to the vehicle group ($p < 0.001$) (fig. 2B). In PTX-treated cells, phosphorylation levels of ERK1/2 were increased after 30-minute treatment with either AM1710 or CP55940 ($p < 0.001$) (fig. 2B).

Similarly, CP55940 (1μM final concentration) and AM1710 (1μM final concentration) both induced ERK1/2 phosphorylation in HEK cells stably expressing hCB2 ($F_{3, 8} = 109.2$, $p < 0.001$) and the level of phosphorylated ERK1/2 changed over time ($F_{4, 32} = 286.8$, $p < 0.001$) (fig. 2C). The significant interaction between treatment and time ($F_{12, 32} = 107.6$, $p < 0.001$) indicates that the ERK1/2 phosphorylation induced by CP55940 and AM1710 was also time dependent. Specifically, both CP55940 and AM1710 induced rapid ERK1/2 phosphorylation at 5 minutes ($p <$

Molecular Pharmacology Fast Forward. Published on November 30, 2018 as DOI: 10.1124/mol.118.113233
This article has not been copyedited and formatted. The final version may differ from this version.

0.001), followed by a reduction in phosphorylation and then an increase at 30 minutes, which was greater for CP55940 ($p < 0.001$) (fig. 2C). No difference in ERK1/2 phosphorylation was observed between basal and vehicle conditions ($p = 1$) (fig. 2C). After PTX pretreatment, CP55940 and AM1710 affected ERK1/2 phosphorylation levels in very distinct ways ($F_{3, 8} = 50.01$, $p < 0.001$ [treatment]; $F_{3, 24} = 160.3$, $p < 0.001$ [time]; $F_{9, 24} = 58.5$, $p < 0.001$ [interaction]) (fig. 2D). AM1710 induced rapid dephosphorylation of ERK1/2 relative to the vehicle group at 5 ($p < 0.001$) and 10 ($p = 0.007$) minutes, and then slightly increased phosphorylation of ERK1/2 at 30 minutes ($p < 0.001$). By contrast, CP55940 induced delayed ERK1/2 phosphorylation at 30 minutes only ($p < 0.001$) (fig. 2D). The total ERK1/2 levels did not differ among treatments over time in cells stably expressed mCB2 ($F_{3, 8} = 0.267$, $p = 0.848$ [treatment]; $F_{4, 32} = 0.965$, $p = 0.440$ [time]; $F_{12, 32} = 0.546$, $p = 0.868$ [interaction]) (fig. 2E) or hCB2 ($F_{3, 8} = 0.481$, $p = 0.704$ [treatment]; $F_{4, 32} = 1.114$, $p = 0.367$ [time]; $F_{12, 32} = 1.034$, $p = 0.443$ [interaction]) (fig. 2F).

AM1710 Phosphorylated JNK 46/54 similarly in HEK Cells Expressing mCB2 or hCB2.

In HEK cells stably expressing mCB2, overall, the phosphorylation of JNK 46/54 changed over time ($F_{4, 32} = 18.86$, $p < 0.001$) (fig. 3A). Both CP55940 and AM1710 increased JNK 46/54 phosphorylation ($F_{3, 8} = 17.4$, $p < 0.001$), which was time dependent ($F_{12, 32} = 7.813$, $p < 0.001$) (fig. 3A). Specifically, AM1710 increased JNK 46/54 phosphorylation at 5 ($p < 0.001$) and 10 minutes ($p < 0.001$), whereas CP55940 activated JNK 46/54 phosphorylation at 5 minutes ($p = 0.002$) (fig. 3A). No differences were observed between vehicle and basal conditions ($p > 0.266$) (fig. 3A). Similarly, both CP55940 and AM1710 activated the phosphorylation of JNK 46/54 in HEK cells stably expressing hCB2 ($F_{12, 32} = 7.813$, $p < 0.001$ [treatment]; $F_{12, 32} = 7.813$, $p < 0.001$ [time]; $F_{12, 32} = 7.813$, $p < 0.001$ [interaction]) (fig. 3B). AM1710 increased JNK 46/54 phosphorylation at 5 ($p = 0.001$), and CP55940 activated JNK 46/54 phosphorylation at 5 ($p < 0.001$) and 10 minutes ($p = 0.002$). No differences were observed between vehicle and basal conditions ($p > 0.357$) (fig. 3B).

Molecular Pharmacology Fast Forward. Published on November 30, 2018 as DOI: 10.1124/mol.118.113233
This article has not been copyedited and formatted. The final version may differ from this version.

Prior History of Chronic AM1710 Treatment Suppresses Paclitaxel-Induced Allodynia and Delays the Development of Tolerance to the Anti-Allodynic Effects of Morphine

Paclitaxel (4 mg/kg, i.p.), administered on four alternate days, induced neuropathic pain in mice, as indicated by the reduction in the mechanical withdrawal threshold ($F_{1, 21}$ = 544.316, p <0.001) (fig. 4A) and increase in the response time to cold stimulation ($F_{1, 21}$ = 204.137, p <0.001) (fig. 4B). No group difference was observed ($F_{2, 21}$ = 0.644, p = 0.535 [mechanical]; $F_{2, 21}$ = 0.284, p = 0.755 [cold]) in mechanical or cold responsiveness prior to pharmacological manipulations. An interaction between paclitaxel treatment and groups was detected for mechanical paw withdrawal threshold ($F_{2, 21}$ = 4.463, p = 0.024), although Bonferroni post hoc tests failed to detect any significant pairwise comparisons, suggesting that mechanical paw withdrawal thresholds did not differ between groups prior to Phase I dosing. The interaction between chemotherapy treatment and groups for cold sensitivity was not significant ($F_{2, 21}$ = 1.489, p = 0.248). Thus, groups were similar prior to initiating drug treatments.

To study the effects of AM1710 pretreatment on the development of tolerance to morphine, pharmacological manipulations were employed in two phases of treatment during the maintenance of neuropathic pain, when neuropathic pain was established and stable. AM1710 (5 mg/kg/day i.p. x 12 days), administered once daily for 12 consecutive days to paclitaxel-treated WT mice during Phase I, increased mechanical paw withdrawal thresholds ($F_{2, 21}$ = 74.940, p < 0.001) (fig. 4A) and reduced the heightened cold response time ($F_{2, 21}$ = 52.339, p = 0.001) (fig. 4B) compared to the vehicle treatment. Mechanical and cold sensitivity returned to the baseline level measured before paclitaxel injection (p = 0.521 [mechanical], p = 0.374 [cold]; planned comparison between baseline 1 (BL1) and day 1 of Phase I, paired t test). The anti-allodynic effect of AM1710 did not differ as a function of time ($F_{6, 63}$ = 1.176, p = 0.33 [mechanical]; $F_{6, 63}$ = 1.301, p = 0.270 [cold]). Mechanical paw withdrawal thresholds ($F_{3, 63}$ = 3.329, p = 0.025, Bonferroni post hoc test did not reveal any differences) and cold response times ($F_{3, 63}$ = 1.189, p = 0.321) remained stable throughout Phase I treatment, indicating that tolerance did not develop

Molecular Pharmacology Fast Forward. Published on November 30, 2018 as DOI: 10.1124/mol.118.113233
This article has not been copyedited and formatted. The final version may differ from this version.

to the anti-allodynic effects of AM1710 over repeated administration for either stimulus modality (fig. 4A & B).

On day 15, three days after the completion of Phase I of AM1710 treatment, mechanical and cold hypersensitivity returned back to the level of hypersensitivity detected before AM1710 treatment ($p = 0.230$ [mechanical], $p = 0.630$ [cold]; planned comparison between baseline 2 (BL2) and Pac in fig. 4A & B, paired t test). Chronic administration of morphine (10 mg/kg/day i.p. x 12 days) was then initiated in Phase II on day 16. Overall, repeated morphine dosing in Phase II reduced mechanical ($F_{3, 60} = 53.59$, $p < 0.001$) and cold ($F_{3, 60} = 32.45$, $p < 0.001$) responsiveness in paclitaxel-treated mice, but the mechanical paw withdrawal threshold ($F_{2, 20} = 19.746$, $p < 0.001$) and cold response time ($F_{2, 20} = 11.049$, $p = 0.001$) differed between groups. Mechanical and cold sensitivity in each group varied differently over repeated morphine administration ($F_{6, 60} = 20.34$, $p < 0.001$ [mechanical]; $F_{6, 60} = 15.271$, $p < 0.001$ [cold]). Specifically, morphine reduced mechanical ($p < 0.001$) and cold ($p < 0.001$) responsiveness in paclitaxel-treated mice relative to the vehicle group on the first day (day 16) of morphine treatment (fig. 4A & B). However, by day 19, morphine was no longer efficacious in reducing paclitaxel-induced hypersensitivities in vehicle (I)-morphine(II)-treated groups, consistent with the development of morphine tolerance (fig. 4A & B). By contrast, morphine suppressed responsiveness to both modalities of cutaneous stimulation ($p < 0.001$ mechanical; $p = 0.015$ cold) on day 19 in paclitaxel-treated mice that received AM1710 (I)-morphine (II) treatment, although efficacy disappeared by day 23 (fig. 4A & B). These results indicate that prior history of AM1710 treatment delayed the development of tolerance to morphine.

Naloxone-Precipitated Opioid Withdrawal was Decreased in Morphine-Tolerant Mice with a Prior History of AM1710 Treatment

We also evaluated whether prior chronic treatment with AM1710 (5 mg/kg i.p. x 12 days) in Phase I would impact naloxone-precipitated morphine withdrawal symptoms in mice rendered tolerant to morphine (10 mg/kg i.p. x 12 days) in Phase II. The number of naloxone-precipitated

Molecular Pharmacology Fast Forward. Published on November 30, 2018 as DOI: 10.1124/mol.118.113233
This article has not been copyedited and formatted. The final version may differ from this version.

jumps differed reliably between groups ($F_{2, 19} = 7.264$, $p = 0.0045$; one way ANOVA). Paclitaxel-treated mice that received vehicle (I)-morphine (II) treatment exhibited a greater number of jumps compared to vehicle (I)-vehicle (II)-treated mice that never received morphine ($p = 0.002$; Bonferroni's post hoc test) (fig. 5A). Moreover, naloxone-precipitated jumps did not differ between the AM1710 pretreatment (i.e. AM1710 (I)-morphine (II)) and vehicle (i.e. vehicle (I)-vehicle (II)) groups ($p = 0.188$; Bonferroni post hoc-test) (fig. 5A). The number of naloxone-precipitated jumps was lower in the AM1710 (I)-morphine (II)) group compared to the vehicle (I)-morphine (II) group that received identical morphine treatments (p = 0.042; Bonferroni's multiple comparison test). These observations suggest that AM1710 attenuated naloxone-precipitated withdrawal jumps in morphine-dependent mice and that withdrawal jumping was normalized by AM1710 pretreatment.

AM1710 did not alter effects of naloxone challenge on body weight or body temperature. Body weight decreased over time after naloxone injection ($F_{1, 19} = 36.052$, $p < 0.001$), which was independent of the treatment ($F_{2, 19} = 0.626$, $p = 0.546$), and weight loss did not differ among treatments ($F_{2, 19} = 0.219$, $p = 0.806$) (fig. 5B). Similarly, no differences were observed between treatments with respect to changes in body temperature induced by naloxone challenge ($F_{2, 21} = 1.390$, $p = 0.273$) (fig. 5C).

AM1710 Does Not Precipitate Cannabinoid CB1 Receptor-Mediated Withdrawal

In mice chronically treated with Δ^9-THC (50 mg/kg/day i.p. x 9 days), pharmacological challenge (2nd challenge) increased the number of each withdrawal parameters relative to the earlier vehicle challenge (1st challenge) of the same mice ($F_{1, 10} = 15.093$, $p = 0.003$ [paw tremor]; $F_{1, 10} = 5.729$, $p = 0.038$ [head shakes]; $F_{1, 10} = 10.07$, $p = 0.01$ [grooming]; $F_{1, 10} = 14.259$, $p = 0.004$ [rearing]) (fig. 6). Challenge with the CB1 antagonist rimonabant elicited more withdrawal behaviors than challenge with AM1710 ($F_{1, 10} = 16.426$, $p = 0.002$ [paw tremor]; $F_{1, 10} = 8.13$, $p = 0.017$ [head shakes]; $F_{1, 10} = 19.659$, $p = 0.001$ [grooming]; $F_{1, 10} = 19.552$, $p = 0.001$ [rearing]), and this effect was phase-dependent ($F_{1, 10} = 15.910$, $p = 0.003$ [paw tremor]; $F_{1, 10} = 9.027$, $p = 0.013$ [head shakes]; $F_{1, 10} = 6.224$, $p = 0.032$ [grooming]; $F_{1, 10} = 16.821$, $p = 0.002$ [rearing]). Bonferroni post

Molecular Pharmacology Fast Forward. Published on November 30, 2018 as DOI: 10.1124/mol.118.113233
This article has not been copyedited and formatted. The final version may differ from this version.

hoc tests revealed no difference in the withdrawal behaviors after early vehicle challenge, but later rimonabant challenge induced greater numbers of each withdrawal behavior relative to AM1710 challenge (p <0.05) (fig. 6). Moreover, rimonabant challenge produced more withdrawal behaviors compared to the early vehicle challenge of the same animals (p <0.01) (fig. 6). By contrast, AM1710 challenge did not elicit more withdrawal behaviors compared with the earlier vehicle challenge in the same animals (p > 0.05), indicating that AM1710 at 10 mg/kg did not precipitate CB1-receptor-mediated withdrawal (fig. 6).

AM1710 Does Not Suppress Mechanical Allodynia in Mice in the CFA Model

Both WT and CB2 KO mice developed mechanical hypersensitivity after intradermal CFA injection as indicated by the observed reduction of the mechanical paw withdrawal threshold ($F_{1, 14}$ = 175.769, p < 0.001) (fig. 7A). The degree of reduction in mechanical withdrawal threshold induced by CFA was similar between WT and CB2 KO mice ($F_{1, 14}$ = 0.012, p = 0.915), and no interaction between group and CFA injection was observed ($F_{1, 14}$ = 0.888, p = 0.362). After the establishment of CFA-induced inflammatory pain, doses of AM1710 (0, 1, 3, 10 mg/kg, i.p.) that reversed paclitaxel-induced neuropathic pain ((Deng, Guindon, *et al.*, 2015); see also fig. 4A and B) did not reverse CFA-induced mechanical hypersensitivity ($F_{3, 42}$ = 2.165, p = 0.106). The lack of anti-allodynic efficacy of AM1710 was observed in both WT and CB2 KO mice ($F_{1, 14}$ = 0.834, p = 0.376), and the interaction between the dose of AM1710 and genotype was not significant ($F_{3, 42}$ = 1.344, p = 0.273). By contrast, the positive control gabapentin reversed CFA-induced mechanical hypersensitivity relative to the vehicle treatment in WT mice as shown in fig. 7B ($F_{3, 30}$ = 19.009, p<0.001 [dose]; $F_{1, 10}$ = 9.210, p = 0.01 [group]; $F_{3, 30}$ = 4.168, p = 0.014 [interaction]). The gabapentin-induced reversal of mechanical hypersensitivity was dose-dependent as revealed by Bonferroni post hoc tests. Specifically, gabapentin at a dose of 30 and 100 mg/kg increased mechanical withdrawal thresholds compared to the vehicle group (p <0.01) and compared to the lower dose of 3 and 10 mg/kg (p <0.05).

Molecular Pharmacology Fast Forward. Published on November 30, 2018 as DOI: 10.1124/mol.118.113233
This article has not been copyedited and formatted. The final version may differ from this version.

We further investigated the effect of prophylactic chronic treatment with AM1710 (10 mg/kg/day x 12 days, i.p.) on CFA-induced mechanical allodynia in WT mice. Chronic AM1710 treatment was initiated 30 minutes before the CFA injection on day 1 and continued once daily for 12 consecutive days (i.e. until day 12). Pre-emptive AM1710 treatment before CFA injection did not prevent the development of mechanical allodynia induced by CFA as the mechanical threshold declined 24 hours after the CFA injection on day 2 ($F_{1, 9} = 75.709$, $p < 0.001$) independent of the treatment ($F_{1, 9} = 0.911$, $p = 0.365$) and mechanical thresholds did not differ between groups ($F_{1, 9} = 1.013$, $p = 0.340$). During the subsequent chronic treatment with AM1710 (i.e. day 2-day 12), mechanical paw withdrawal thresholds varied over time ($F_{5, 45} = 4.892$, $p = 0.001$) independent of the treatment ($F_{5, 45} = 0.209$, $p = 0.957$) but mechanical responsiveness did not differ between the AM1710 and vehicle-treated groups ($F_{1, 9} = 0.482$, $p = 0.505$) (fig. 7C), suggesting a lack of anti-allodynic efficacy of AM1710. By contrast, gabapentin treatment 30 minutes before CFA injection successfully prevented the development of mechanical allodynia induced by CFA; mechanical paw withdrawal thresholds were reduced on day 2 in the vehicle treated-mice ($p = 0.001$) but not in gabapentin-treated mice ($p = 0.810$). Mechanical paw withdrawal thresholds changed over time during subsequent gabapentin chronic treatment from day 2 to day 8 ($F_{3, 30} = 3.168$, $p = 0.039$), but post hoc comparisons did not reveal any significant differences across days. The observation of group differences in CFA-induced mechanical sensitivity ($F_{1, 10} = 40.718$, $p < 0.001$) between vehicle- and gabapentin-treated groups were independent of time ($F_{3, 30} = 1.081$, $p = 0.372$), implies a sustained gabapentin-induced suppression of CFA-induced mechanical hypersensitivity throughout the testing period compared to the vehicle group (fig. 7D).

AM1710 Does Not Suppress Mechanical or Cold Allodynia in the PSNL Model

PSNL decreased mechanical paw withdrawal thresholds ($F_{1, 10} = 27.434$, $p < 0.001$) in a manner independent of the genotype ($F_{1, 10} = 1.437$, $p = 0.258$) (fig. 8A) and neuropathic pain developed similarly in WT and CB2 KO mice ($F_{1, 10} = 0.000253$, $p = 0.988$). After the establishment of PSNL-induced neuropathic pain, a main effect of AM1710 treatment was detected (0, 1, 3, 10

Molecular Pharmacology Fast Forward. Published on November 30, 2018 as DOI: 10.1124/mol.118.113233
This article has not been copyedited and formatted. The final version may differ from this version.

mg/kg, i.p.) ($F_{3, 30}$ = 3.487, p = 0.028), but Bonferroni post hoc tests failed to reveal any differences between these doses. Moreover, no difference in responsiveness was detected between WT and CB2 KO mice ($F_{1, 10}$ = 0.001, p = 0.975) and responsiveness was independent of the doses ($F_{3, 30}$ = 1.129, p = 0.353), suggesting lack of antinociceptive efficacy of AM1710 in the PSNL model. By contrast, in WT mice, gabapentin increased mechanical paw withdrawal thresholds relative to the vehicle group as shown in fig. 8B ($F_{3, 30}$ = 15.420, p < 0.001 [dose]; $F_{1, 10}$ = 24.134, p = 0.001 [group]; $F_{3, 30}$ = 10.996, p < 0.001 [interaction]). Gabapentin produced significant reversal of mechanical allodynia at doses of 30 and 50 mg/kg compared to either the vehicle group (p <0.001) or lower doses of gabapentin (i.e. 3 and 10 mg/kg i.p.; p <0.05) (fig. 8B).

CP55940 Does Not Suppress Mechanical or Cold Allodynia in CB1KOs in CFA or PSNL Models

Because of the lack of robust anti-allodynic efficacy of AM1710 in PSNL and CFA models, we asked whether CB2-mediated anti-allodynic effects could be observed in these two models using a different, functionally balanced cannabinoid agonist, CP55940. In AtT20 cells expressing mCB2, CP55940 inhibits voltage-gated calcium channels whereas AM1710 fails to do so (Atwood *et al.*, 2012; Dhopeshwarkar and Mackie, 2016). Both CP55940 and AM1710 inhibit cyclase and recruit arrestin with similar efficacy (Dhopeshwarkar and Mackie, 2016). We, consequently, evaluated the anti-allodynic effect of CP55940 using CB1 KO mice to eliminate unwanted motor effects associated with activation of CB1 that would otherwise mask detection of CB2-mediated anti-allodynic effects (Deng, Cornett, *et al.*, 2015).

Intradermal CFA injection lowered mechanical paw withdrawal thresholds in CB1 KO mice ($F_{1, 5}$ = 97.925, p < 0.001) in a manner that was selective for the CFA-injected (ipsilateral) paw ($F_{1, 5}$ = 12.915, p = 0.016). As expected, mechanical paw withdrawal thresholds were lower in the ipsilateral compared to contralateral ($F_{1, 5}$ = 25.457, p = 0.004) paw. Intraplantar injection of CFA decreased the mechanical paw withdrawal threshold in the ipsilateral paw of CB1 KO mice (p < 0.001), but did not alter responding in the non-inflamed (contralateral) paw (p = 0.512) (fig. 9A).

Molecular Pharmacology Fast Forward. Published on November 30, 2018 as DOI: 10.1124/mol.118.113233
This article has not been copyedited and formatted. The final version may differ from this version.

CP55940, at increasing doses (0, 3, 10 mg/kg, i.p.) was not able to reverse CFA-induced mechanical hypersensitivity ($F_{2, 10} = 1.209$, $p = 0.339$). Moreover, mechanical paw withdrawal thresholds were lower in the ipsilateral compared to the contralateral paw of the same mice ($F_{1, 5} = 335.290$, $p < 0.001$) and this effect was independent of the dose of CP55940 ($F_{2, 10} = 0.288$, $p = 0.756$). Thus, CP55940 did not alleviate the CFA-induced allodynia in CB1 KO mice (fig. 9A).

PSNL decreased mechanical paw withdrawal thresholds ($F_{1, 6} = 54.17$, $p < 0.001$) (fig. 9B) and increased cold response durations ($F_{1, 6} = 20.747$, $p = 0.004$) (fig. 9C) in CB1 KO mice. The changes in mechanical and cold sensitivity were selective for the paw ipsilateral to traumatic nerve injury ($F_{1, 6} = 307.932$, $p < 0.001$ [mechanical]; $F_{1, 6} = 15.469$, $p = 0.008$ [cold]). Mechanical paw withdrawal threshold and cold responsiveness was lower in the ipsilateral compared to the contralateral paw ($F_{1, 6} = 35.828$, $p = 0.001$ [mechanical]; $F_{1, 6} = 20.148$, $p = 0.004$ [cold]) (fig. 9B&C). PSNL surgery lowered mechanical paw withdrawal threshold ($p < 0.001$) and increased cold sensitivity ($p < 0.001$) in the ipsilateral (i.e. injured) paw without altering responsiveness in the contralateral (un-injured) paw ($p = 0.330$ [mechanical], $p = 0.325$ [cold]) (fig. 9B&C). CP55940 (0, 3, 10 mg/kg, i.p.) did not produce a robust anti-allodynic efficacy in mice subjected to PSNL ($F_{2, 12} = 2.147$, $p = 0.160$ [mechanical]; $F_{2, 12} = 0.375$, $p = 0.695$ [cold]). Mechanical paw withdrawal thresholds ($F_{1, 6} = 110.775$, $p < 0.001$) were lower and cold sensitivity ($F_{1, 6} = 41.852$, $p = 0.001$) was greater in the ipsilateral compared to the contralateral side, and these responses were not impacted by CP55940 dose ($F_{2, 12} = 1.528$, $p = 0.256$ [mechanical]; $F_{2, 12} = 0.383$, $p = 0.690$ [cold]) (fig. 9B&C), indicating lack of anti-allodynic efficacy of CP55940 in PSNL of CB1 KO mice.

DISCUSSION

Opioid tolerance and physical dependence limit clinical use for treating chronic pain (Volkow *et al.*, 2018). Here we show that chronic pretreatment with the CB2 agonist AM1710 delayed, but did not eliminate, development of morphine tolerance in paclitaxel-treated mice. These observations correspond with the ability of the G protein-biased CB2 agonist LY2828360 to block

development of antinociceptive tolerance to morphine in paclitaxel-treated WT but not CB2 KO mice (Lin *et al.*, 2017). Anti-allodynic effects of AM1710 are absent in CB2 KO and preserved in CB1 KO mice (Deng, Guindon, *et al.*, 2015), validating its use as a CB2 agonist in the present studies. In HEK cells expressing mCB2, both AM1710 (present study) and LY2828360 (Lin *et al.*, 2017) inhibit adenylyl cyclase and activate ERK1/2, albeit with different time courses. However, LY2828360 does not internalize CB2 receptors or recruit beta-arrestin (Lin *et al.*, 2017), in contrast to AM1710 (Atwood *et al.*, 2012; Dhopeshwarkar and Mackie, 2016). CB2 agonists may diminish morphine tolerance to different degrees, depending on the agonist and its signaling profile, although mediation by CB2 has not been consistently assessed. In tumor-bearing rats, the CB2 agonist AM1241 blocked morphine analgesic tolerance in the hot plate test, but not in assessments of mechanical allodynia (Zhang *et al.*, 2016). JWH-015 potentiated morphine antinociception and antinociceptive tolerance, although mediation by CB2 was not assessed (Altun *et al.*, 2015). By contrast, the putative CB2 antagonist JTE907 reduced morphine's antinociceptive efficacy and tolerance (Altun *et al.*, 2015). Different agonists, pain states, and/or off-target effects could account for differences between studies.

Morphine-induced glial activation and release of proinflammatory factors oppose morphine antinociception may contribute to morphine tolerance; conversely, inhibition of glial activation or proinflammatory cytokine actions reduces morphine analgesic tolerance (for review see Watkins *et al.*, 2005, 2009). Interestingly, deletion of mu opioid receptor (MOR), which is absent in microglia, from nociceptors abrogates development of morphine tolerance without disrupting analgesia (Corder *et al.*, 2017). CB2 antibodies are not sufficiently robust to be used for immunohistochemical localization. Nonetheless, CB2 mRNA is detected in microglia and their levels increase under pathological conditions, reviewed in (Guindon and Hohmann, 2008; Atwood and Mackie, 2010). Thus, microglial CB2 activation may counter-regulate morphine-induced glial activation and release of proinflammatory cytokines. The minimally-selective cannabinoid agonist JWH-015 attenuated morphine-induced increases in microglial proinflammatory mediators,

Molecular Pharmacology Fast Forward. Published on November 30, 2018 as DOI: 10.1124/mol.118.113233
This article has not been copyedited and formatted. The final version may differ from this version.

possibly via a CB2/Akt-ERK1/2 signaling pathway (Merighi *et al.*, 2012). Anti-inflammatory signaling via CB2 in immune cells (Galiegue *et al.*, 1995) could oppose morphine tolerance by decreasing pro-inflammatory mediators (Grace *et al.*, 2015). In tumor-bearing rats, AM1241 increased MOR expression in spinal cord and DRG (Zhang *et al.*, 2016).

AM1710 suppressed naloxone-precipitated opioid withdrawal in paclitaxel-treated mice and normalized naloxone-precipitated jumping to control levels. Similarly, LY2828360 (I)-morphine (II) treatment trended to reduce naloxone-precipitated opioid withdrawal in our previous report (Lin *et al.*, 2017). Upregulation of adenylyl cyclase has been linked to mechanisms of opioid dependence (Bohn *et al.*, 2000). Thus, CB2-mediated inhibition of adenylyl cyclase by either AM1710 or LY2828360 may counteract morphine-induced adenylyl cyclase upregulation to attenuate morphine withdrawal.

In vitro, AM1710 exhibits higher affinity to CB2 compared to CB1 (Khanolkar *et al.*, 2007), but is a low potency inverse agonist/antagonist at CB1(Dhopeshwarkar *et al.*, 2017). Our observation that a CB1 antagonist enhanced anti-allodynic efficacy of a CB2 agonist (Rahn *et al.*, 2008) fostered medicinal chemistry efforts that led to development of AM1710. CB1 antagonism could enhance selectivity of mixed ligands that bind preferentially to CB2 over CB1 and limit CB1-mediated side effects.. Nonetheless, in Δ^9-THC-tolerant mice, challenge with rimonabant, but not AM1710, precipitated cannabinoid CB1-dependent withdrawal. Thus, CB1 antagonism observed *in vitro* did not translate to functionally relevant CB1 antagonism *in vivo*.

In our study, AM1710 (1-10 mg/kg, i.p.) did not suppress allodynia induced by PSNL or CFA. Moreover, prophylactic chronic treatment with AM1710 did not attenuate development of CFA-induced mechanical allodynia. Thus, lack of efficacy of AM1710 cannot be attributed to different stages in development of inflammatory nociception. Nonetheless, AM1710 (5 mg/kg, i.p.) suppressed paclitaxel-induced allodynia without tolerance in the present study and in our previously work (Rahn *et al.*, 2014; Deng, Guindon, *et al.*, 2015). CFA, PSNL and paclitaxel produce mechanistically distinct pain states which may contribute to differences between studies.

Molecular Pharmacology Fast Forward. Published on November 30, 2018 as DOI: 10.1124/mol.118.113233
This article has not been copyedited and formatted. The final version may differ from this version.

AM1710 attenuates neuropathic allodynia produced by mechanistically distinct chemotherapeutic agents (Deng *et al.*, 2012) and produces CB2-mediated suppressions of paclitaxel-induced allodynia in both mice (Deng, Guindon, *et al.*, 2015) and rats (Deng *et al.*, 2012; Rahn *et al.*, 2014). In rats, intrathecal AM1710 reversed mechanical allodynia induced by chronic constriction injury or human immunodeficiency virus-1 glycoprotein 120 (Wilkerson *et al.*, 2012), although mediation by CB2 was not assessed. The exact mechanisms underlying anti-allodynic efficacy of AM1710 in paclitaxel-induced neuropathic pain are unknown. As a microtubule-interfering agent, paclitaxel activates the c-Jun N-terminal kinase/stress-activated protein kinase (JNK/SAPK) signaling pathway (Wang *et al.*, 1998). However, there is no direct causal link between paclitaxel-induced activation of JNK and paclitaxel-induced peripheral neuropathic pain. In our studies, AM1710 induced phosphorylation of JNK 46/54 in HEK cells stably expressing mCB2 and hCB2. JNK may be activated in different cells by paclitaxel and AM1710. Both acute AM1710 (one injection 5 mg/kg, i.p.) and chronic AM1710 (5 mg/kg/day i.p. x 8 days) reduced mRNA levels of monocyte chemoattractant protein 1 (MCP-1) and TNF-α (Deng, Guindon, *et al.*, 2015) in lumbar spinal cord of paclitaxel-treated mice. The inhibitory effect of AM1710 on these pro-inflammatory cytokines may underlie its anti-allodynic efficacy in the paclitaxel model.

Other putative CB2 agonists suggested to exhibit anti-allodynic effects in CFA model are GW405833 (Li *et al.*, 2017), AM1241 (Hsieh *et al.*, 2011; Gao *et al.*, 2016), A836339 (Yao *et al.*, 2009; Hsieh *et al.*, 2011), GW842166X (Giblin *et al.*, 2007), and A-796260 (Yao *et al.*, 2008). However, most studies have not thoroughly evaluated pharmacological specificity in vivo. Strikingly, the putative CB2 agonist GW405833, which does not produce cardinal signs of CB1 activation in the tetrad, suppressed mechanical allodynia in CFA and PSNL model in mice through CB1 but not CB2 mechanisms (Li *et al.*, 2017). Anti-allodynic effects of GW405833 in CFA and PSNL models were fully preserved in CB2 KO mice and absent in CB1 KO mice, and were blocked by a CB1 but not a CB2 antagonist (Li *et al.*, 2017). The other ligands noted above were evaluated in rats and most studies did not evaluate mechanical allodynia. Interestingly,

Molecular Pharmacology Fast Forward. Published on November 30, 2018 as DOI: 10.1124/mol.118.113233
This article has not been copyedited and formatted. The final version may differ from this version.

JWH133 shows antinociceptive efficacy in the PSNL model following intrathecal but not systemic (i.p.) administration (Yamamoto et al., 2008). These observations led us to ask another question: to what extent is CB2-mediated antinociceptive efficacy observed in CFA and PSNL models in mice. Our lab previously showed that high doses of CP55940 (3-10 mg/kg, i.p.) produced sustained CB2-mediated suppression of paclitaxel-induced allodynia in CB1 KO mice; these anti-allodynic effects were blocked by the CB2 antagonist AM630 (Deng, Cornett, *et al.*, 2015). However, CP55940 (3, 10 mg/kg, i.p.) did not suppress CFA or PSNL-induced mechanical allodynia in CB1 KO mice in the present study. These observations suggest that AM1710 is not a broad spectrum analgesic and is only efficacious in certain pain models.

Modest differences in the signaling profile of AM1710 were observed between mCB2 and hCB2 for inhibition of cAMP and activation of ERK1/2. For example, AM1710 induced early and brief inhibition of cAMP levels by mCB2, but induced a delayed and long lasting inhibition of cAMP levels by hCB2. Moreover, AM1710 induced early and long lasting of ERK1/2 phosphorylation by mCB2, but only transiently increased phosphorylated ERK1/2 by hCB2. Thus, caution must be exerted when translating in vivo results from mice to humans. By contrast, AM1710 activation of JNK signaling by mCB2 and hCB2 were similar. In contrast to the AM1710-induced early inhibition of adenylyl cyclase levels and early activation of ERK1/2 phosphorylation starting at 5 minutes, LY282360 only showed delayed inhibition of cAMP at 30 minutes and delayed activation of ERK1/2 phosphorylation starting at 20 minutes (Lin *et al.*, 2017). AM1710 displays functional selectivity distinct from LY2828360. AM1710 internalized CB2 and recruited β-arrestin2 (Atwood *et al.*, 2012; Dhopeshwarkar and Mackie, 2016), but only weakly activated MAPK and did not inhibit voltage gated calcium channel (VGCC) (Atwood *et al.*, 2012). By contrast, LY2828360 did not recruit arrestin and failed to internalize CB2 (Lin et al., 2017). Differences in the signaling profiles of AM1710 and LY2828360 likely contribute to agonist differences in ability to inhibit development morphine tolerance, because AM1710 delayed whereas LY2828360 completely blocked morphine tolerance (Lin et al., 2017).

Molecular Pharmacology Fast Forward. Published on November 30, 2018 as DOI: 10.1124/mol.118.113233
This article has not been copyedited and formatted. The final version may differ from this version.

In conclusion, AM1710 delayed the development of morphine tolerance in paclitaxel-treated mice and reduced naloxone-precipitated opioid withdrawal. AM1710 did not produce functionally-relevant CB1 antagonism *in vivo*. AM1710 suppressed paclitaxel-induced mechanical and cold allodynia, but failed to suppress mechanical allodynia induced by either CFA or PSNL. The balanced cannabinoid agonist CP55940 similarly failed to suppress allodynia in either the CFA or PSNL models in CB1 KO mice. Modest species differences were detected in signaling of AM1710 at mouse and human CB2. These observations should be considered when selecting appropriate therapeutic indications for CB2 agonists for clinical translation.

Molecular Pharmacology Fast Forward. Published on November 30, 2018 as DOI: 10.1124/mol.118.113233
This article has not been copyedited and formatted. The final version may differ from this version.

AUTHOR CONTRIBUTIONS

Participated in research design: Hohmann and Mackie.

Conducted experiments: Li, Lin, Thomaz, Carey, and Dhopeshwarkar.

Contributed new reagents or analytic tools: Makriyannis, Nikas, and Liu.

Performed data analysis: Li, Lin, Thomaz, Carey, and Hohmann.

Wrote or contributed to the writing of the manuscript: Li, Lin, Thomaz, Carey, Dhopeshwarkar Hohmann, and Mackie.

References

Altun A, Yildirim K, Ozdemir E, Bagcivan I, Gursoy S, and Durmus N (2015) Attenuation of morphine antinociceptive tolerance by cannabinoid CB1 and CB2 receptor antagonists. *J Physiol Sci* **65**:407–415, Springer Japan.

Atwood BK, and Mackie K (2010) CB 2: A cannabinoid receptor with an identity crisis. *Br J Pharmacol* **160**:467–479.

Atwood BK, Wager-miller J, Haskins C, Straiker A, and Mackie K (2012) Functional Selectivity in CB 2 Cannabinoid Receptor Signaling and Regulation : Implications for the Therapeutic Potential of. 250–263.

Beltramo M, Bernardini N, Bertorelli R, Campanella M, Nicolussi E, Fredduzzi S, and Reggiani A (2006) CB2 receptor-mediated antihyperalgesia: Possible direct involvement of neural mechanisms. *Eur J Neurosci* **23**:1530–1538.

Bingham B, Jones PG, Uveges AJ, Kotnis S, Lu P, Smith VA, Sun SC, Resnick L, Chlenov M, He Y, Strassle BW, Cummons TA, Piesla MJ, Harrison JE, Whiteside GT, and Kennedy JD (2007) Species-specific in vitro pharmacological effects of the cannabinoid receptor 2 (CB2) selective ligand AM1241 and its resolved enantiomers. *Br J Pharmacol* **151**:1061–1070.

Bohn LM, Gainetdinov RR, Lin F-T, Lefkowitz RJ, and Caron MG (2000) μ-Opioid receptor desensitization by β-arrestin-2 determines morphine tolerance but not dependence. *Nature* **408**:720–723.

Brown SM, Wager-Miller J, and Mackie K (2002) Cloning and molecular characterization of the rat CB2 cannabinoid receptor. *Biochim Biophys Acta* **1576**:255–264.

Corder G, Tawfik VL, Wang D, Sypek EI, Low SA, Dickinson JR, Sotoudeh C, Clark JD, Barres A, Bohlen CJ, and Scherrer G (2017) Loss of μ-opioid receptor signaling in nociceptors, and not spinal microglia, abrogates morphine tolerance without disrupting analgesic efficacy. *Nat*

Med **23**:164–173.

Deng L, Cornett BL, Mackie K, and Hohmann AG (2015) CB1 knockout mice unveil sustained CB2-mediated antiallodynic effects of the mixed CB1/CB2 agonist CP55,940 in a mouse model of paclitaxel-induced neuropathic pain. *Mol Pharmacol* **88**:64–74.

Deng L, Guindon J, Cornett BL, Makriyannis A, Mackie K, and Hohmann AG (2015) Chronic cannabinoid receptor 2 activation reverses paclitaxel neuropathy without tolerance or cannabinoid receptor 1-dependent withdrawal. *Biol Psychiatry* **77**:475–487, Elsevier.

Deng L, Guindon J, Vemuri VK, Thakur G a., White F a., Makriyannis A, and Hohmann AG (2012) The maintenance of cisplatin- and paclitaxel-induced mechanical and cold allodynia is suppressed by cannabinoid CB2 receptor activation and independent of CXCR4 signaling in models of chemotherapy-induced peripheral neuropathy. *Mol Pain* **8**:71.

Dhopeshwarkar A, and Mackie K (2016) Functional Selectivity of CB2 Cannabinoid Receptor Ligands at a Canonical and Noncanonical Pathway. *J Pharmacol Exp Ther* **358**:342–351.

Dhopeshwarkar A, Murataeva N, Makriyannis A, Straiker A, and Mackie KP (2017) Two Janus cannabinoids that are both CB2 agonists and CB1 antagonists. *J Pharmacol Exp Ther* **360**:300–311.

Felder CC, Joyce KE, Briley EM, Mansouri J, Mackie K, Blond O, Lai Y, Ma AL, and Mitchell RL (1995) Comparison of the pharmacology and signal transduction of the human cannabinoid CB1 and CB2 receptors. *Mol Pharmacol* **48**:443–450.

Galiegue S, Mary S, Marchand J, Dussossoy D, Carriere D, Carayon P, Bouaboula M, Shire D, Le Fur G, and Casellas P (1995) Expression of Central and Peripheral Cannabinoid Receptors in Human Immune Tissues and Leukocyte Subpopulations. *Eur J Biochem* **232**:54–61.

Gao F, Zhang L-H, Su T-F, Li L, Zhou R, Peng M, Wu C-H, Yuan X-C, Sun N, Meng X-F, Tian B,

Shi J, Pan H-L, and Li M (2016) Signaling Mechanism of Cannabinoid Receptor-2 Activation-Induced β-Endorphin Release. *Mol Neurobiol* **53**:3616–3625, Springer US.

Giblin GMP, O'Shaughnessy CT, Naylor A, Mitchell WL, Eatherton AJ, Slingsby BP, Rawlings DA, Goldsmith P, Brown AJ, Haslam CP, Clayton NM, Wilson AW, Chessell IP, Wittington AR, and Green R (2007) Discovery of 2-[(2,4-Dichlorophenyl)amino]-N-[(tetrahydro- 2H-pyran-4-yl)methyl]-4-(trifluoromethyl)- 5-pyrimidinecarboxamide, a Selective CB2 Receptor Agonist for the Treatment of Inflammatory Pain. , doi: 10.1021/JM061195+, American Chemical Society.

Grace PM, Maier SF, and Watkins LR (2015) Opioid-Induced central immune signaling: Implications for opioid analgesia. *Headache* **55**:475–489.

Griffin G, Tao Q, and Abood ME (2000) Cloning and Pharmacological Characterization of the Rat CB 2 Cannabinoid Receptor 1. *J Pharmacol Exp Ther* **292**:886–894.

Guindon J, and Hohmann AG (2008) Cannabinoid CB2 receptors: a therapeutic target for the treatment of inflammatory and neuropathic pain. *Br J Pharmacol* **153**:319–334.

Herkenham M, Lynn AB, Johnson MR, Melvin LS, de Costa BR, and Rice KC (1991) Characterization and localization of cannabinoid receptors in rat brain: a quantitative in vitro autoradiographic study. *J Neurosci* **11**:563–83.

Hsieh GC, Pai M, Chandran P, Hooker BA, Zhu CZ, Salyers AK, Wensink EJ, Zhan C, Carroll WA, Dart MJ, Yao BB, Honore P, and Meyer MD (2011) Central and peripheral sites of action for CB2 receptor mediated analgesic activity in chronic inflammatory and neuropathic pain models in rats. *Br J Pharmacol* **162**:428–440.

Khanolkar AD, Lu D, Ibrahim M, Duclos RI, Thakur GA, Malan TP, Porreca F, Veerappan V, Tian X, George C, Parrish DA, Papahatjis DP, and Makriyannis A (2007) Cannabilactones: A novel class of CB2 selective agonists with peripheral analgesic activity. *J Med Chem*

50:6493–6500.

Li A-L, Carey LM, Mackie K, and Hohmann AG (2017) The cannabinoid CB $_2$ agonist GW405833 suppresses inflammatory and neuropathic pain through a CB $_1$ mechanism that is independent of CB $_2$ receptors in mice. *J Pharmacol Exp Ther* jpet.117.241901.

Lin X, Dhopeshwarkar AS, Huibregtse M, Mackie K, and Hohmann AG (2017) The slowly signaling G protein-biased CB2 cannabinoid receptor agonist LY2828360 suppresses neuropathic pain with sustained efficacy and attenuates morphine tolerance and dependence. *Mol Pharmacol* mol.117.109355.

Malan TP, Ibrahim MM, Lai J, Vanderah TW, Makriyannis A, and Porreca F (2003) CB2 cannabinoid receptor agonists: Pain relief without psychoactive effects? *Curr Opin Pharmacol* **3**:62–67.

Matsuda LA, Bonner TI, and Lolait SJ (1993) Localization of cannabinoid receptor mRNA in rat brain. *J Comp Neurol* **327**:535–550.

Merighi S, Gessi S, Varani K, Fazzi D, Mirandola P, and Borea PA (2012) Cannabinoid CB2 receptor attenuates morphine-induced inflammatory responses in activated microglial cells. *Br J Pharmacol* **166**:2371–2385.

Mukherjee S, Adams M, Whiteaker K, Daza A, Kage K, Cassar S, Meyer M, and Yao BB (2004) Species comparison and pharmacological characterization of rat and human CB2cannabinoid receptors. *Eur J Pharmacol* **505**:1–9.

Patel S, Naeem S, Kesingland A, Froestl W, Capogna M, Urban L, and Fox A (2001) The effects of GABA(B) agonists and gabapentin on mechanical hyperalgesia in models of neuropathic and inflammatory pain in the rat. *Pain* **90**:217–226.

Pertwee RG (2001) Cannabinoid receptors and pain. *Prog Neurobiol* **63**:569–611.

Rahn EJ, Deng L, Thakur GA, Vemuri K, Zvonok AM, Lai YY, Makriyannis A, and Hohmann AG (2014) Prophylactic cannabinoid administration blocks the development of paclitaxel-induced neuropathic nociception during analgesic treatment and following cessation of drug delivery. *Mol Pain* **10**:1–19, Molecular Pain.

Rahn EJ, Thakur GA, Wood JAT, Zvonok AM, Makriyannis A, and Hohmann AG (2011) Pharmacological characterization of AM1710, a putative cannabinoid CB2agonist from the cannabilactone class: Antinociception without central nervous system side-effects. *Pharmacol Biochem Behav* **98**:493–502, Elsevier Inc.

Rahn EJ, Zvonok AM, Thakur G a, Khanolkar AD, Makriyannis A, and Hohmann AG (2008) Selective activation of cannabinoid CB2 receptors suppresses neuropathic nociception induced by treatment with the chemotherapeutic agent paclitaxel in rats. *J Pharmacol Exp Ther* **327**:584–591.

Volkow N, Benveniste H, and McLellan AT (2018) Use and Misuse of Opioids in Chronic Pain. *Annu Rev Med* **69**:annurev-med-011817-044739.

Wang T, Wang H, Ichijo H, Giannakakou P, Foster JS, Fojo T, and Wimalasena J (1998) Microtubule-interfering Agents Activate c-Jun N-terminal Kinase / Stress-activated Protein Kinase through Both Ras and Apoptosis Signal-regulating Kinase Pathways *. **273**:4928–4936.

Watkins LR, Hutchinson MR, Johnston IN, and Maier SF (2005) Glia: Novel counter-regulators of opioid analgesia. *Trends Neurosci* **28**:661–669.

Watkins LR, Hutchinson MR, Rice KC, and Maier SF (2009) The “Toll” of Opioid-Induced Glial Activation: Improving the Clinical Efficacy of Opioids by Targeting Glia. *Trends Pharmacol Sci* **30**:581–591.

Wilkerson JL, Gentry KR, Dengler EC, Wallace JA, Kerwin AA, Armijo LM, Kuhn MN, Thakur GA,

Makriyannis A, and Milligan ED (2012) Intrathecal cannabilactone CB 2R agonist, AM1710, controls pathological pain and restores basal cytokine levels. *Pain* **153**:1091–1106, International Association for the Study of Pain.

Yao BB, Hsieh G, Daza A V, Fan Y, Grayson GK, Garrison TR, El Kouhen O, Hooker BA, Pai M, Wensink EJ, Salyers AK, Chandran P, Zhu CZ, Zhong C, Ryther K, Gallagher ME, Chin CL, Tovcimak AE, Hradil VP, Fox GB, Dart MJ, Honore P, and Meyer MD (2009) Characterization of a cannabinoid CB2 receptor-selective agonist, A-836339 [2,2,3,3-tetramethyl-cyclopropanecarboxylic acid [3-(2-methoxy-ethyl)-4,5-dimethyl-3H-thiazol-(2Z)-ylidene]-amide], using in vitro pharmacological assays, in vivo pain models, and . *J Pharmacol Exp Ther* **328**:141–151.

Yao BB, Hsieh GC, Frost JM, Fan Y, Garrison TR, Daza A V, Grayson GK, Zhu CZ, Pai M, Chandran P, Salyers a K, Wensink EJ, Honore P, Sullivan JP, Dart MJ, and Meyer MD (2008) In vitro and in vivo characterization of A-796260: a selective cannabinoid CB2 receptor agonist exhibiting analgesic activity in rodent pain models. *Br J Pharmacol* **153**:390–401.

Yekkirala AS, Roberson DP, Bean BP, and Woolf CJ (2017) Breaking barriers to novel analgesic drug development. *Nat Rev Drug Discov* **16**:545–564, Nature Publishing Group.

Zhang J, Hoffert C, Vu HK, Groblewski T, Ahmad S, and O'Donnell D (2003) Induction of CB2 receptor expression in the rat spinal cord of neuropathic but not inflammatory chronic pain models. *Eur J Neurosci* **17**:2750–2754.

Zhang M, Wang K, Ma M, Tian S, Wei N, and Wang G (2016) Low-dose cannabinoid type 2 receptor agonist attenuates tolerance to repeated morphine administration via regulating μ-opioid receptor expression in walker 256 tumor-bearing rats. *Anesth Analg* **122**:1031–1037.

Zimmermann M (1983) Ethical guidelines for investigations of experimental pain in conscious animals. *Pain* **16**:109–10.

Footnotes

Conflict of Interest

AM is a consultant for MAK Scientific. KM is a consultant for Renew and Abalone. None of the other author(s) declare potential conflicts of interest with respect to the research, authorship, and/or publication of this article.

Financial Support

The author(s) disclosed receipt of the following financial support for the research, authorship, and/or publication of this article: This work was supported by National Institute on Drug Abuse [Grant DA041229, DA045020, DA009158, DA021696]; and National Cancer Institute [Grant CA200417]. LMC is supported by National Institute on Drug Abuse [T32 Grant DA024628] and the Harlan Research Summer Scholars program.

Molecular Pharmacology Fast Forward. Published on November 30, 2018 as DOI: 10.1124/mol.118.113233
This article has not been copyedited and formatted. The final version may differ from this version.

Figure legends

Figure 1. AM1710 inhibited forskolin-stimulated cAMP in HEK cells expressing mCB2 and hCB2, but the kinetics of inhibition differed between mCB2 and hCB2. A. In HEK cells expressing mCB2**,** both CP55940 and AM1710 reduced cAMP levels at 5 minutes. The inhibitory effect of AM1710 lasted longer than CP55940 and dissipated by 15 minutes. **B**. After treating HEK cells expressing mCB2 with PTX, both CP55940 and AM1710 failed to reduce cAMP levels at all time points examined. **C**. In HEK cells expressing hCB2, CP55940 induced early reduction of cAMP at 5 minutes which lasted up to 10 minutes, whereas AM1710 induced a delayed (at 10 minutes) but long lasting (up to 30 minutes) decrease in cAMP. **D**. After treating HEK cells expressing hCB2 with PTX, both CP55940 and AM1710 failed to reduce cyclase levels at all time points examined. * $p < 0.05$vs. No Fsk; $^{\#}p < 0.05$ vs. Veh + Fsk, ^$p < 0.05$ significant difference between CP + Fsk and AM1710 + Fsk(Two-Way Mixed ANOVA, followed by Bonferroni's post hoc test). mCB2: mouse CB2 receptors; hCB2: human CB2 receptors; Veh: vehicle; Fsk: forskolin; CP: CP55940 N=3 for each group.

Figure 2. AM1710 activated CB2 receptor- and G protein-dependent ERK1/2 phosphorylation in HEK cells expressing mCB2 and hCB2, but the kinetics of inhibition differed between mCB2 and hCB2. A. In HEK cells expressing mCB2**,** AM1710 consistently induced ERK1/2 phosphorylation at all time points examined whereas CP55940 biphasically increased ERK1/2 phosphorylation.. **B**. After treating HEK cells expressing mCB2 with PTX, both CP55940 and AM1710 failed to induce ERK1/2 phosphorylation except at 30 minutes. Interestingly, by contrast, CP55940 reduced ERK1/2 phosphorylation at 5 minutes after PTX treatment. **C**. In HEK cells expressing hCB2, both CP55940 and AM1710 induced rapid phosphorylation of ERK1/2 at 5 minutes, followed by reduction of ERK1/2 phosphorylation and increase of phosphorylation at 30 minutes. **D**. After treating HEK cells expressing hCB2 with PTX, AM1710 reduced ERK1/2 phosphorylation at the 5- and 10- minute time points, while slightly increasing ERK1/2 phosphorylation at 30 minutes. CP55940 showed only activation of

Molecular Pharmacology Fast Forward. Published on November 30, 2018 as DOI: 10.1124/mol.118.113233
This article has not been copyedited and formatted. The final version may differ from this version.

ERK1/2 phosphorylation at 30 minutes. Total ERK1/2 levels did not differ between conditions in HEK cells expressing mCB2 (**E**) or hCB2 (**F**). * $p < 0.05$ vs. vehicle; ^$p < 0.05$ significant difference between CP55940 and AM1710 (Two-Way Mixed ANOVA, followed by Bonferroni's post hoc test). mCB2: mouse CB2 receptors; hCB2: human CB2 receptors. N=3 for each group.

Figure 3. AM1710 increased phosphorylation of JNK 46/54 similarly in HEK cells stably expressing mCB2 and hCB2. A. In HEK cells stably expressing mCB2, AM1710 increased phosphorylation of JNK 46/54 at 5 and 10 minutes, CP55940 increased phosphorylation of JNK 46/54 only at 5 minutes. **B.** In HEK cells stably expressing hCB2, AM1710 increased phosphorylation of JNK 46/54 at 5 minutes, CP55940 increased phosphorylation of JNK 46/54 at 5 and 10 minutes. * $p < 0.05$ vs. Vehicle; $^{\#}p < 0.05$ significant difference between CP55940 and AM1710. N=3 for each group.

Figure 4. AM1710 sustainably suppressed paclitaxel-induced allodynia and delayed the development of morphine antinociceptive tolerance in mice. C57BL/J6 mice received a total of four doses of paclitaxel (4 mg/kg, i.p.) to develop peripheral neuropathic pain. After the paclitaxel-induced neuropathic pain was fully established, AM1710 (5 mg/kg/day x 12 days) alone was administered during phase I. And four days after AM1710 administration, animals received chronic treatment of morphine (10 mg/kg/day x 12 days) alone during phase II. AM1710 sustainably suppressed mechanical (**A**) and cold (**B**) allodynia induced by paclitaxel during phase I. The history of AM1710 treatment during phase I delayed the development of morphine tolerance in phase II. n = 8 male C57BL/6J for each group. $^{\#}$ $p < 0.05$ vs. BL (baseline); * $p < 0.05$ vs. Veh (I) – Veh (II); ^ $p < 0.05$ vs. day 23 (Two-Way Mixed ANOVA, followed by Bonferroni's post hoc test). Veh: vehicle; MPH: morphine; BL: baseline.

Figure 5. AM1710 attenuates naloxone-precipitated opioid withdrawal. Paclitaxel-treated mice rendered tolerant to morphine were challenged with naloxone (5 mg/kg, i.p.) to induce physical withdrawal. (**A**) Animals pretreated with AM1710 (5 mg/kg/day x 12 days, i.p.) before morphine (MPH) treatment (10 mg/kg, i.p.) for 12 days exhibited less jumping behavior compared

Molecular Pharmacology Fast Forward. Published on November 30, 2018 as DOI: 10.1124/mol.118.113233
This article has not been copyedited and formatted. The final version may differ from this version.

with animals receiving morphine alone. (**B**) Weight loss did not differ among treatments. (**C**) Body temperature changes did not differ among treatments. n = 8 male C57BL/6J for each group., $^{**}p <$ 0.01 vs. Veh (I)-Veh (I) (One-Way ANOVA, followed by Bonferroni's post hoc test); $^{\#}p < 0.05$ vs. Vehicle (I)-Morphine (II) (One-Way ANOVA, followed by Bonferroni's multiple comparison test). ^^^ $p < 0.001$ vs. post 30 min (Two-Way mixed ANOVA) Veh: vehicle; MPH: morphine.

Figure 6. AM1710 does not precipitate CB1 receptor-mediated cannabinoid withdrawal. Administration of the CB1 antagonist rimonabant (10 mg/kg, i.p.) increased the number of paw tremors (**A**), headshakes (**B**), grooming (**C**), and rearing behaviors (**D**) in mice chronically treated with Δ^9-THC (50 mg/kg/day x 9 days, i.p.). By contrast, AM1710 (10 mg/kg, i.p.) did not induce these CB1 receptor-mediated withdrawal behaviors. n = 6 male C57BL/6J for each group. $^{\#}p <$ 0.05, $^{\#\#}p < 0.01$, $^{\#\#\#}p < 0.001$ vs. Vehicle; $^{*}p < 0.05$, $^{**}p < 0.01$ vs. AM1710 (Two-Way Mixed ANOVA, followed by Bonferroni's post hoc test). 1st Challenge: vehicle challenge; 2nd challenge: rimonabant or AM1710 challenge.

Figure 7. AM1710 does not suppress mechanical allodynia induced by CFA injection. **A**. Increasing doses of AM1710 (0-10 mg/kg, i.p.) did not reverse CFA-induced mechanical allodynia in either WT or CB2KO after inflammatory pain was fully established (mixed sex, n = 8 C57BL/6J for WT, n = 8 CB2 KO). **B**. Gabapentin (30 and 100 mg/kg, i.p.) suppressed mechanical allodynia in WT mice after CFA-induced inflammatory pain was established. (n = 6 male C57BL/6J for each group). **C**. Prophylactic and chronic treatment of AM1710 starting 30 minutes before CFA injection and continuing up to day 12 did not prevent and suppress mechanical allodynia induced by CFA in WT. (n = 6 male C57BL/6J for AM1710 group; n = 5 male C57BL/6J for vehicle group). **D**. Prophylactic and chronic treatment of gabapentin starting 30 minutes before CFA injection and continuing up to day 8 prevented and sustainably suppressed mechanical allodynia induced by CFA in WT. (n = 6 male C57BL/6J for each group). $^{\#}p < 0.05$ vs. BL (baseline); $^{*}p < 0.05$ vs. vehicle; ^ $p < 0.05$ vs. gabapentin 3 mg/kg (Two-Way Mixed ANOVA, followed by Bonferroni's post hoc test). Black arrow indicates the day when AM1710 (10 mg/kg,

i.p.) or gabapentin (50 mg/kg, i.p.) was injected 30 minutes before the CFA injection. WT: wild type.

Figure 8. AM1710 does not suppress mechanical allodynia induced by PSNL. **A**. AM1710 (0-10 mg/kg, i.p.) did not reverse the mechanical allodynia in either WT or CB2KO after the PSNL-induced neuropathic pain was established (n = 6 male C57BL/6J for WT; n = 6 male for CB2 KO). **B**. Gabapentin (30 and 50 mg/kg, i.p.) significantly suppressed mechanical allodynia once PSNL-induced neuropathic pain was established. (n = 6 male C57BL/6J for each group). $^{\#}$ $p < 0.05$ vs. BL (baseline); * $p < 0.05$ vs. vehicle; ^ $p < 0.05$ vs. gabapentin 3 mg/kg (Two-Way Mixed ANOVA, followed by Bonferroni's post hoc test). BL: baseline.

Figure 9. CP55940 does not suppress allodynia induced by CFA or PSNL in CB1 KO. A. CP55940 (0-10 mg/kg, i.p.) did not suppress mechanical allodynia induced by CFA. (n = 6 male CB1 KO) **B**. Different doses of CP55940 (0-10 mg/kg, i.p.) did not suppress mechanical allodynia induced by PSNL. (n = 7 male CB1 KO). **C**. Different doses of CP55940 (0-10 mg/kg, i.p.) did not suppress cold allodynia induced by PSNL. (n = 7 male CB1 KO). $^{\#}$ $p < 0.05$ vs. BL (baseline); * $p < 0.05$ vs. contralateral side (uninjured side). Two-Way Repeated Measures ANOVA, followed by Bonferroni's post hoc test.

Molecular Pharmacology Fast Forward. Published on November 30, 2018 as DOI: 10.1124/mol.118.113233
This article has not been copyedited and formatted. The final version may differ from this version.

Figure 1

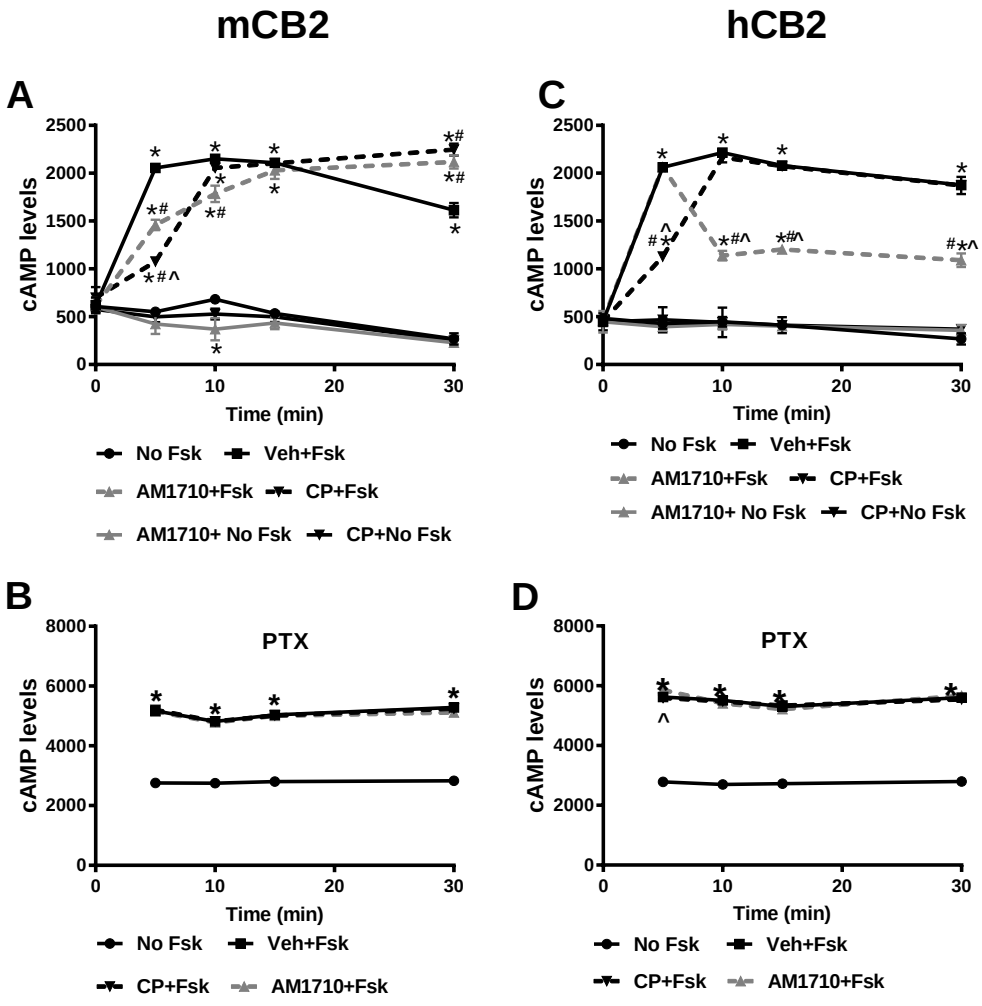

Molecular Pharmacology Fast Forward. Published on November 30, 2018 as DOI: 10.1124/mol.118.113233
This article has not been copyedited and formatted. The final version may differ from this version.

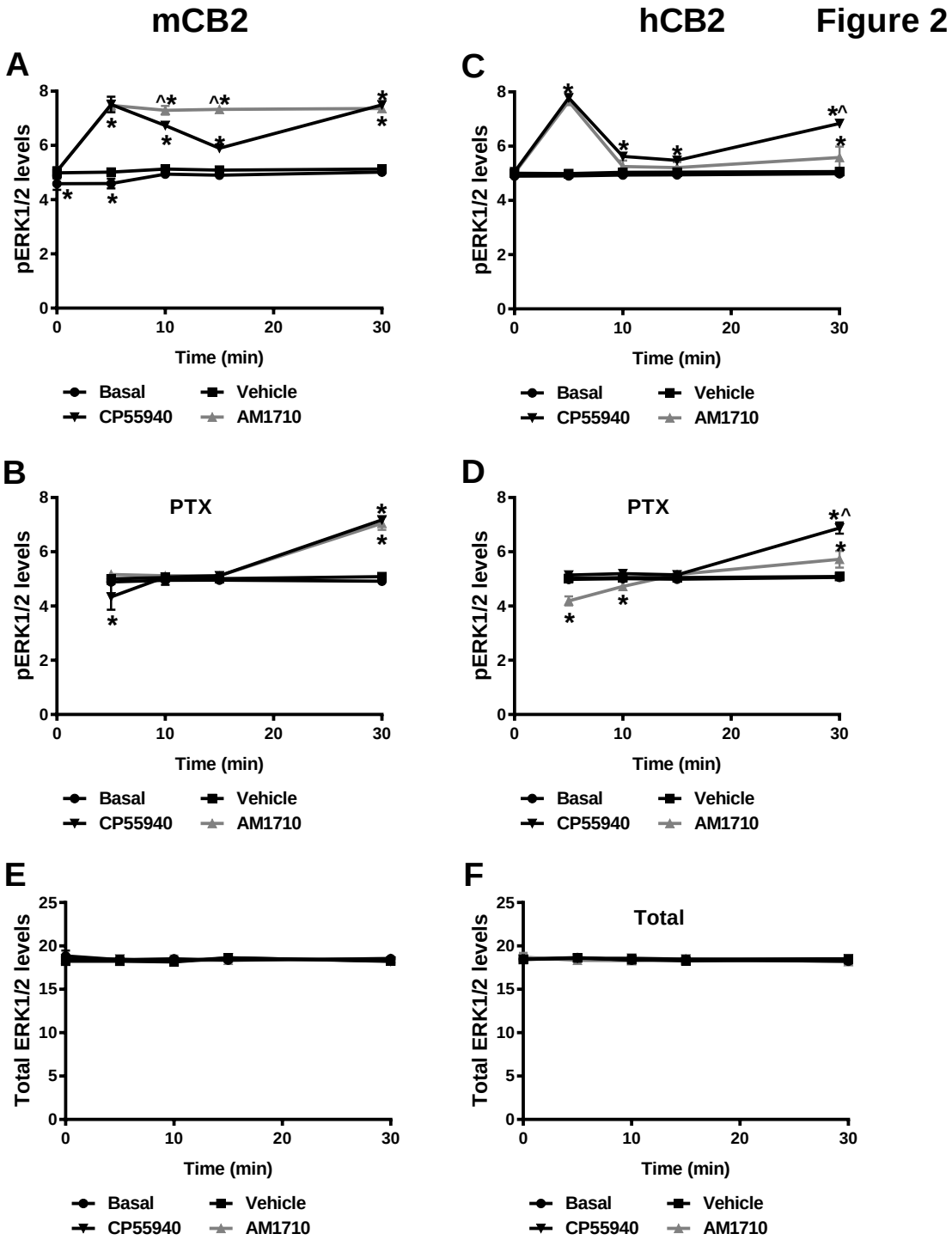

Molecular Pharmacology Fast Forward. Published on November 30, 2018 as DOI: 10.1124/mol.118.113233
This article has not been copyedited and formatted. The final version may differ from this version.

Figure 3

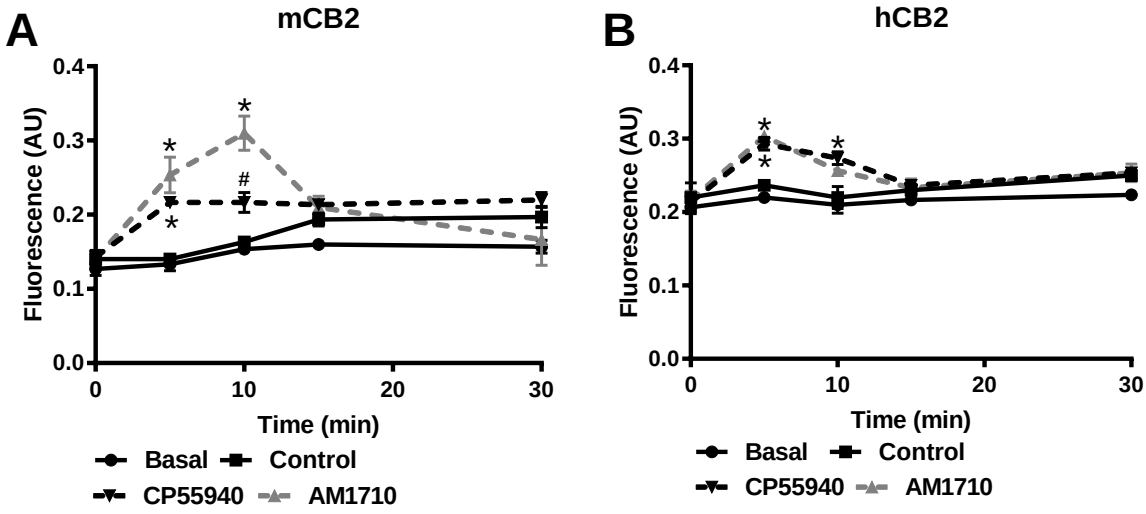

Molecular Pharmacology Fast Forward. Published on November 30, 2018 as DOI: 10.1124/mol.118.113233
This article has not been copyedited and formatted. The final version may differ from this version.

Figure 4

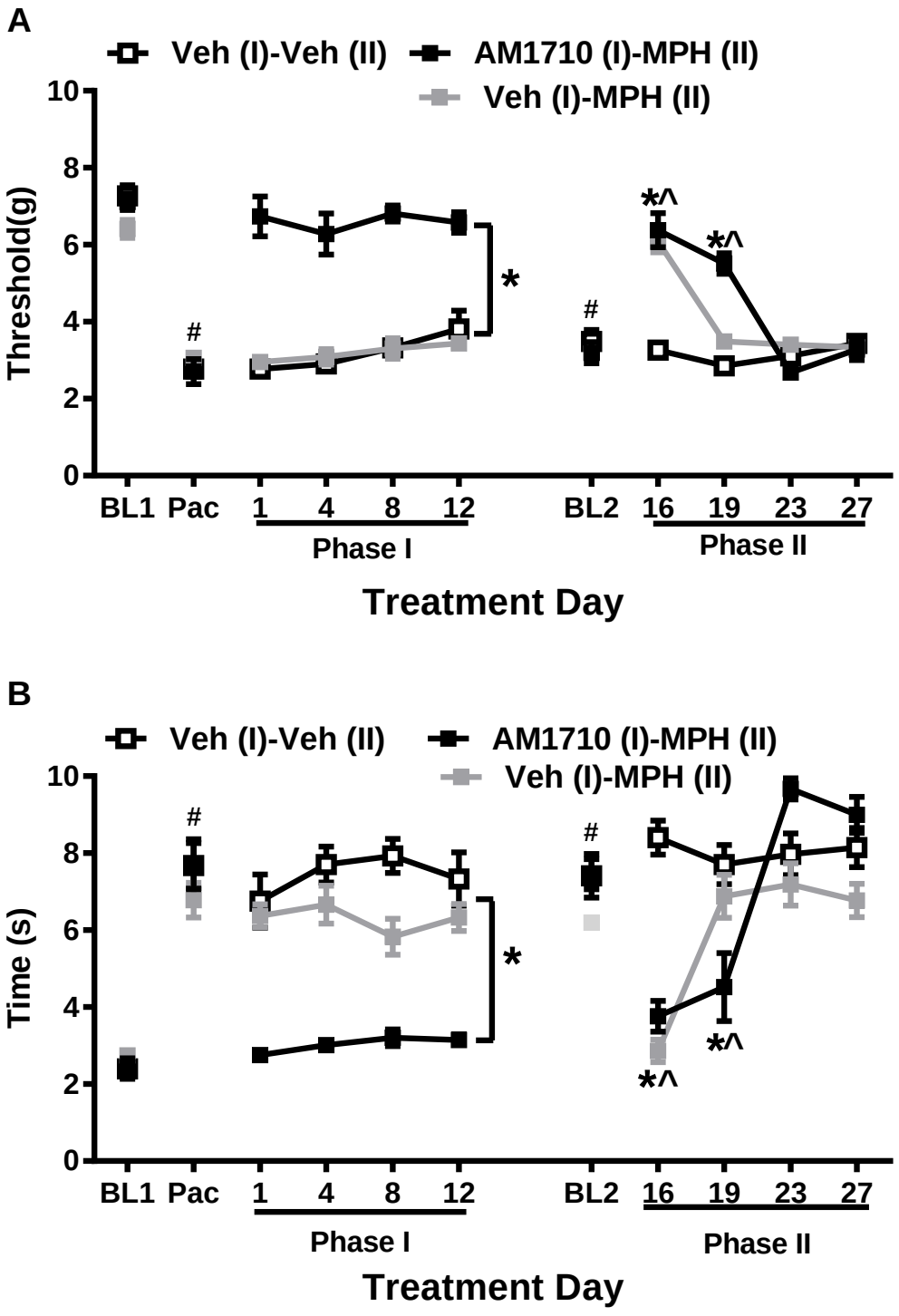

Molecular Pharmacology Fast Forward. Published on November 30, 2018 as DOI: 10.1124/mol.118.113233
This article has not been copyedited and formatted. The final version may differ from this version.

Figure 5

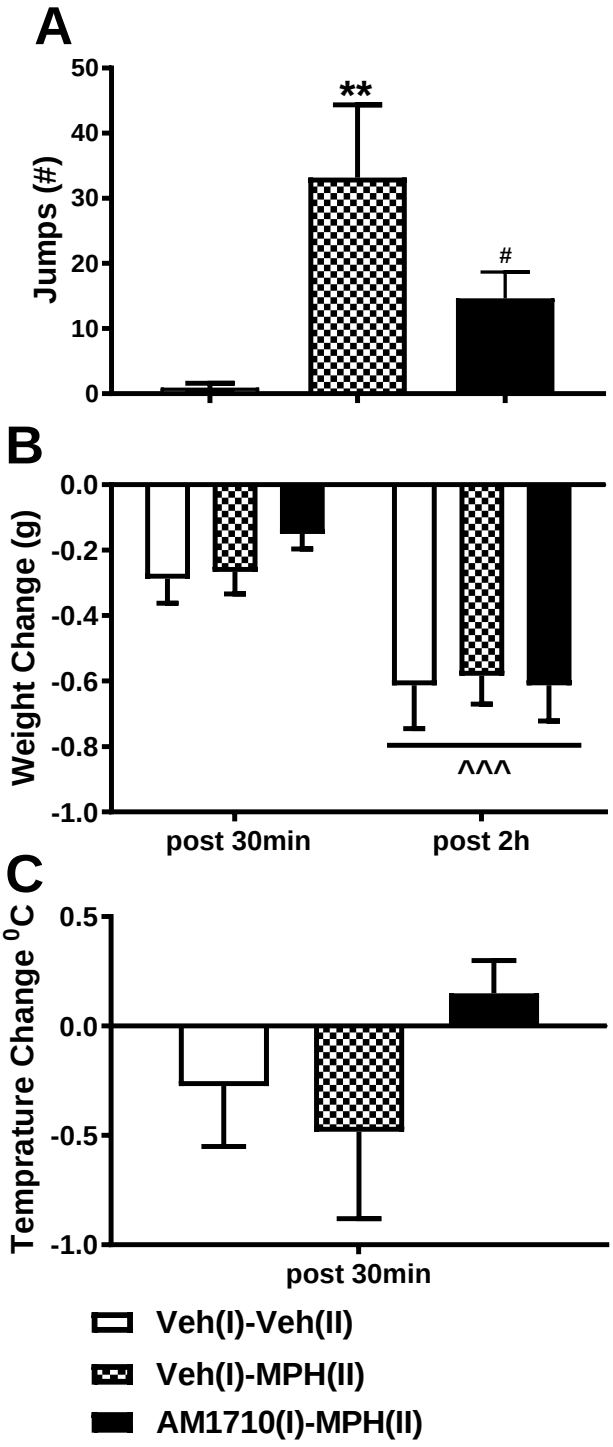

Molecular Pharmacology Fast Forward. Published on November 30, 2018 as DOI: 10.1124/mol.118.113233
This article has not been copyedited and formatted. The final version may differ from this version.

Figure 6

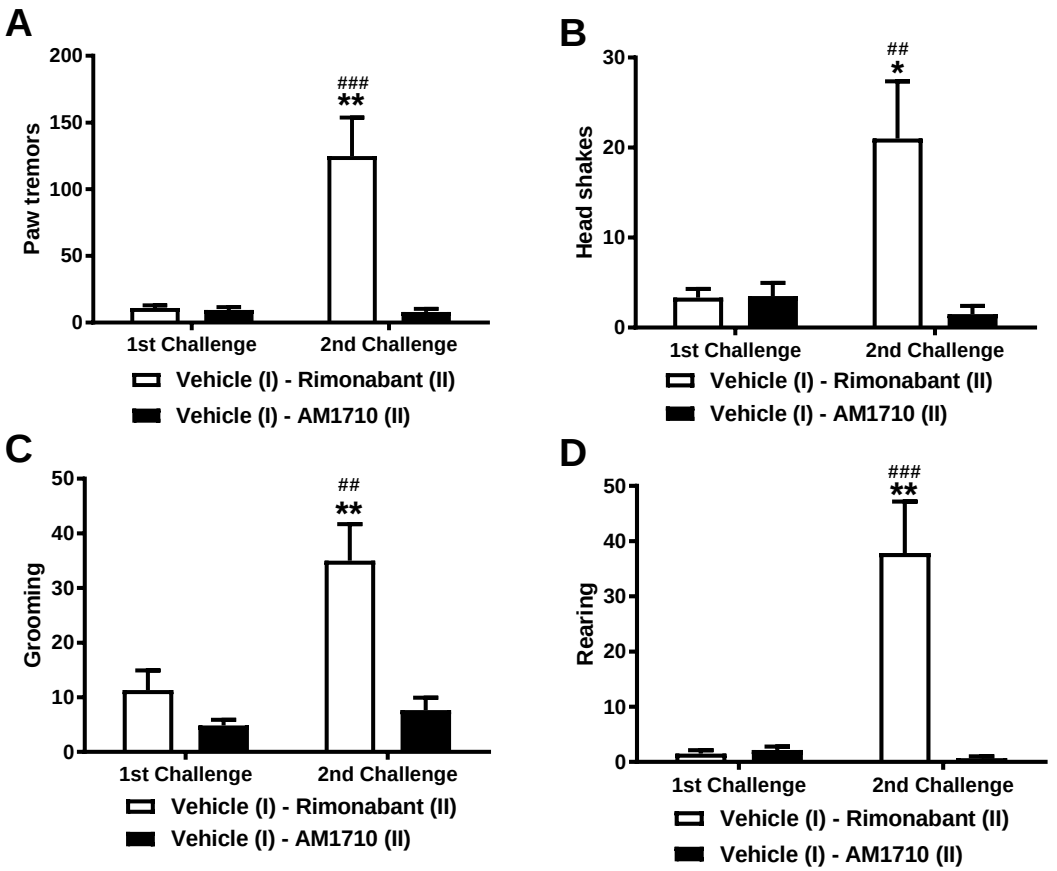

Molecular Pharmacology Fast Forward. Published on November 30, 2018 as DOI: 10.1124/mol.118.113233
This article has not been copyedited and formatted. The final version may differ from this version.

Figure 7

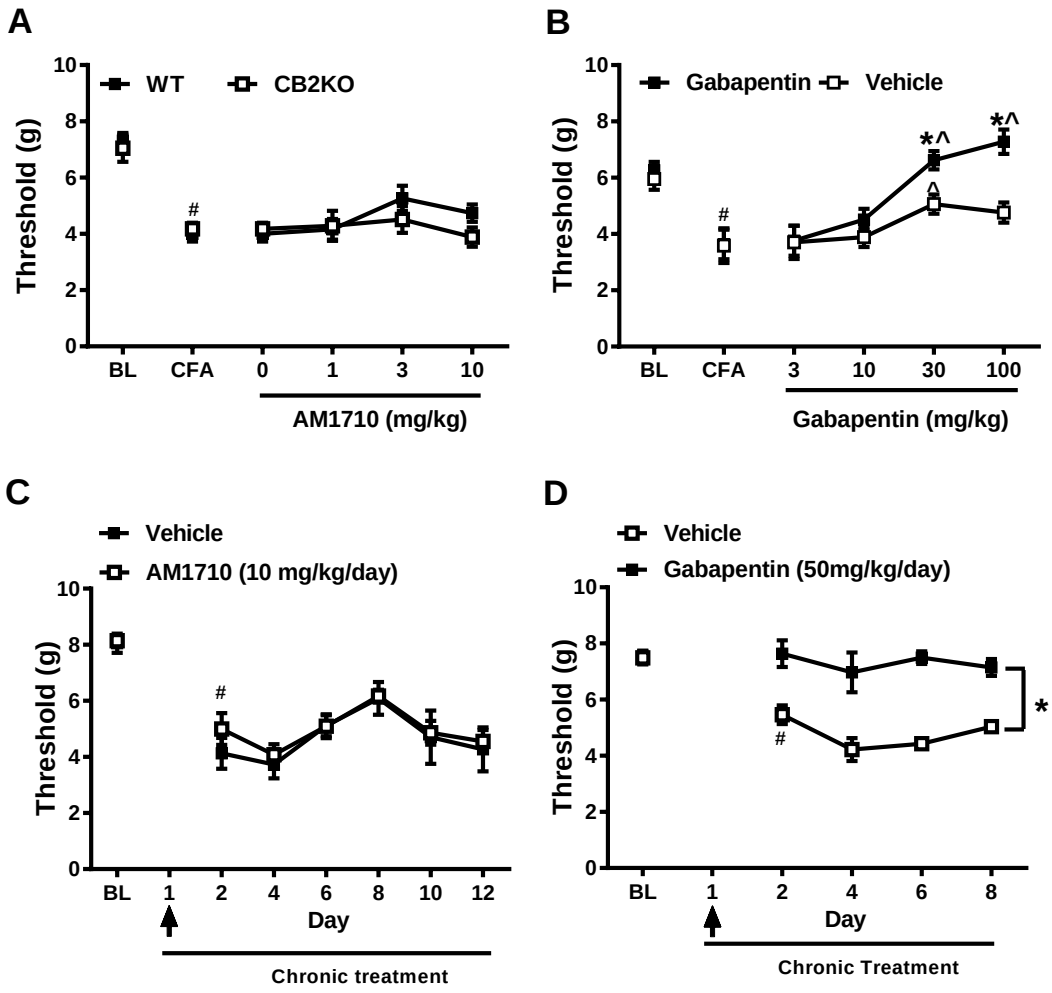

Molecular Pharmacology Fast Forward. Published on November 30, 2018 as DOI: 10.1124/mol.118.113233
This article has not been copyedited and formatted. The final version may differ from this version.

Figure 8

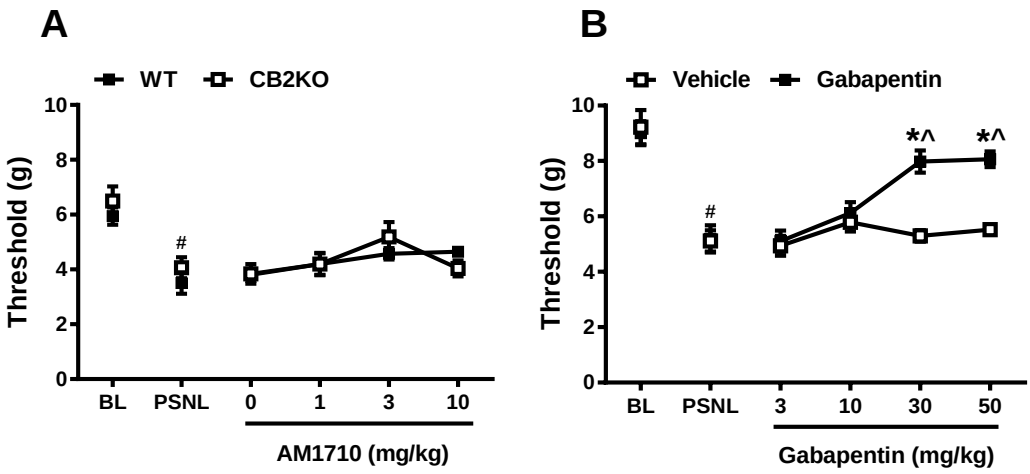

Molecular Pharmacology Fast Forward. Published on November 30, 2018 as DOI: 10.1124/mol.118.113233
This article has not been copyedited and formatted. The final version may differ from this version.

CB1 KO

Figure 9